**A peer-reviewed version of this preprint was published in PeerJ on 25 February 2016.**

View the peer-reviewed version (peerj.com/articles/1637), which is the preferred citable publication unless you specifically need to cite this preprint.

Marycz K, Lewandowski D, Tomaszewski KA, Henry BM, Golec EB, Marędziak M. 2016. Low-frequency, low-magnitude vibrations (LFLM) enhances chondrogenic differentiation potential of human adipose derived mesenchymal stromal stem cells (hASCs) PeerJ 4:e1637 https://doi.org/10.7717/peerj.1637

# Low-frequency, low-magnitude vibrations (LFLM) enhances chondrogenic differentiation potential of human adipose derived mesenchymal stromal stem cells (hASCs)

Krzysztof Marycz, Daniel Lewandowski, Krzysztof A Tomaszewski, Brandon Michael Henry, Edward B Golec, Monika Marędziak

The aim of this study was to evaluate if low-frequency, low-magnitude vibrations (LFLM) could enhance chondrogenic differentiation potential of human adipose derived mesenchymal stem cells (hASCs) with simultaneous inhibition of their adipogenic properties for biomedical purposes. We developed a prototype device that induces low-magnitude (0.3 g) low-frequency vibrations with the following frequencies: 25, 35 and 45 Hz. Afterwards, we used human adipose derived mesenchymal stem cell (hASCS), to investigate their cellular response to the mechanical signals. We have also evaluated hASCs morphological and proliferative activity changes in response to each frequency. Induction of chondrogenesis in hASCs, under the influence of a 35 Hz signal leads to most effective and stable cartilaginous tissue formation through highest secretion of Bone Morphogenetic Protein 2 (BMP-2), and Collagen type II, with low concentration of Collagen type I. These results correlated well with appropriate gene expression level. Simultaneously, we observed significant up-regulation of α3, α4, β1 and β3 integrins in chondroblast progenitor cells treated with 35Hz vibrations, as well as Sox-9. Interestingly, we noticed that application of 35 Hz frequencies significantly inhibited adipogenesis of hASCs. The obtained results suggest that application of LFLM vibrations together with stem cell therapy might be a promising tool in cartilage regeneration.

PeerJ PrePrints | https://dx.doi.org/10.7287/peerj.preprints.1514v1 | CC-BY 4.0 Open Access | rec: 17 Nov 2015, publ: 17 Nov 2015

# Low-frequency, low-magnitude vibrations (LFLM) enhances chondrogenic differentiation potential of human adipose derived mesenchymal stromal stem cells (hASCs).

Krzysztof Marycz [1, 2], Daniel Lewandowski [3], Krzysztof A Tomaszewski [4, 5], Brandon Michael Henry [4], Edward B. Golec [5, 6], Monika Marędziak [7]

1. Faculty of Biology, University of Environmental and Life Sciences, Kozuchowska 5b St, 50-631 Wroclaw, Poland
2. Wroclaw Research Centre EIT +, Stablowicka 147 St, 54-066 Wroclaw, Poland
3. Institute of Materials Science and Applied Mechanics, University of Technology, Smoluchowskiego 25 St, 50-370 Wroclaw, Poland
4. Department of Anatomy, Jagiellonian University Medical College, Kopernika 12 St, 31-034 Krakow, Poland
5. Department of Orthopaedics and Trauma Surgery, 5th Military Clinical Hospital and Polyclinic, Krakow, Poland
6. Faculty of Motor Rehabilitation, Orthopaedic Rehabilitation Department, Bronislaw Czech Academy of Physical Education, Krakow, Poland
7. Faculty of Veterinary Medicine, Department of Animal Physiology and Biostructure University of Environmental and Life Sciences, Norwida 31 St, 50-375 Wroclaw, Poland

**Corresponding author**: Krzysztof Marycz, Electron Microscopy Laboratory, Kożuchowska 5b, 51-631 Wroclaw, Poland , krzysztofmarycz@interia.pl

**Abstract**

The aim of this study was to evaluate if low-frequency, low-magnitude vibrations (LFLM) could enhance chondrogenic differentiation potential of human adipose derived mesenchymal stem cells (hASCs) with simultaneous inhibition of their adipogenic properties for biomedical purposes. We developed a prototype device that induces low-magnitude (0.3 g) low-frequency vibrations with the following frequencies: 25, 35 and 45 Hz. Afterwards, we used human adipose derived mesenchymal stem cell (hASCS), to investigate their cellular response to the mechanical signals. We have also evaluated hASCs morphological and proliferative activity changes in response to each frequency. Induction of chondrogenesis in hASCs, under the influence of a 35 Hz signal leads to most effective and stable cartilaginous tissue formation through highest secretion of Bone Morphogenetic Protein 2 (BMP-2), and Collagen type II, with low concentration of Collagen type I. These results correlated well with appropriate gene expression level. Simultaneously, we observed significant up-regulation of α3, α4, β1 and β3 integrins in chondroblast progenitor cells treated with 35Hz vibrations, as well as Sox-9. Interestingly, we noticed that application of 35 Hz frequencies significantly inhibited adipogenesis of hASCs. The obtained results suggest that application of LFLM vibrations together with stem cell therapy might be a promising tool in cartilage regeneration.

**Keywords:** Low-magnitude low-frequency vibration stimulation, adipose-derived mesenchymal stem cells, chondrogenesis, adipogenesis

## Introduction

Articular cartilage injuries are a growing problem in both human and veterinary medicine. Injury to cartilage manifests through the typical signs of inflammation, and can be caused by either trauma or diseases such as osteonecrosis, cartilage necrosis, or arthritis. Because cartilage is an avascular tissue with chondrocytes that are characterized by a low mitotic potential, the regenerative potential cartilage is substantially limited [1]. As such, the spontaneous regeneration of injured cartilage is extremely difficult. Until recently, the vast majority of the available treatment methods have focused on eliminating symptoms and improving patient quality-of-life through the use steroidal or non-steroidal anti-inflammatory drug treatment (NSAIDs) [2]. However, when used long-term, these medications may lead to chondronecrosis.

A potential solution to this problem emerges in the form of cell based therapies. Adult mesenchymal stem cells (MSCs) may be a possible source of cells for this type of therapy due to their immunomodulatory action, ability to self-renew, and ability to differentiate into several cell lineages, i.e. chondrocytes, osteoblasts or adipocytes [3, 4]. Currently, bone marrow (BMMSCs) and adipose derived mesenchymal stem cells (ASCs) are the cells most frequently applied in cell-based therapies at the preclinical stage. Of the two cell types mentioned above, ASCs seem a better alternative to BMMSCs, due to their easy accessibility, and thus lower donor-related risks [5]. Moreover, activated ASCs secrete from their surface small, spherical membrane fragments called microvesicles (MVs). These MVs contain important regenerative molecules, that improve the function of damaged tissues - eg. growth factors, bioactive lipids, proteins. Microvesicles, secreted by MSCs that have differentiated into osteocytes, release into the culture medium compounds rich in Collagen type I and II or Bone Morphogenetic Protein 2 [6, 7]. Several studies have confirmed the beneficial clinical effect of ASCs in the treatment of musculoskeletal

disorders, particularly in the field of veterinary orthopedics [8, 9, 10]. In our previous study, we demonstrated the positive effects of ASCs application in equine and canine osteoarthritis treatment [11].

However, one major limitation to the clinical application of ASCs is the age-related decrease in the proliferative and chondrogenic differentiation potential of ASCs obtained from older populations [12]. As degenerative joint diseases increase in prevalence with age, it is important to develop methods to overcome this limitation. In order to improve both the proliferative and the differentiation potential of ASCs, various physical stimuli such as static magnetic field [13], electric signals [14] and cyclic strain [15] have been applied. However, this field still remains relatively unexplored in terms of the biological effects of low-magnitude low-frequency vibration (LMLF) - a non-invasive biophysical intervention that leads to cyclic loading of the targeted tissue. LMLF vibrations include values of magnitude under 1.0 g, where g = 9,81 $m/s^2$, and a frequency between 20 – 100 Hz. Several studies have investigated the role of various magnitudes and frequencies of vibrations, such as high-magnitude low-frequency (HMLF) vibrations [16], high-magnitude high frequency vibrations (HMHF) [17] and low-magnitude high-frequency (LMHF) vibrations [18], in the context of their influence on cellular response. Moreover, it has been reported that LMHF enhance the osteogenic differentiation potential of MSCs [18]. Enhancement of osteogenic and/or chondrogenic differentiation potential of MSCs may strongly depend on up-regulation of particular integrins, that are activated by various biomechanical signals. Integrins are heterodimeric glycoproteins that are composed of an α- and a β-subunit, each of which has an extracellular and a cytoplasmic domain [19]. Several studies have provided evidence that chondrocytes express integrins [20-25]. In particular, the α1β1 and α5β1 integrins have been shown to be the most prominent in adult chondrocytes isolated from

normal articular cartilage. However, the other integrins are still poorly investigated, especially in the context of their expression in differentiated precursor cells additionally stimulated by various types of external mechanical or others signals.

In an animal model, LMHF signals had a positive influence on both bone formation and density, enhancing bone strength and recovery after bone fracture [26]. Moreover, preliminary studies in children with disabling conditions and post-menopausal women indicate that such signals can be efficacious in reversing and/or preventing bone loss [26]. However, to the best knowledge of the authors, the current literature lacks data concerning the effects of LMLF vibrations on the chondrogenic differentiation potential of human ASCs.

The aim of this study was to investigate how harmonic vibration, sinusoidal with constant low-magnitude (0.3g, where g = 9,81 $m/s^2$) and low-frequency (25, 35, 45 Hz) mechanical signals, generated by an actuating device, effects ASC morphology, growth, and adipogenic and chondrogenic differentiation potential.

## Materials and Methods

### *Description of the cell vibration generator prototype*

The process of inducing vibrations was carried out using a specially constructed device that allowed to induce mechanical motion of a 24-well culture plate. Movement of the plate was characterized by the harmonic sine of a given amplitude and frequency. The direction of plate translations was perpendicular to the main surface on which the cells were cultured.

A scheme of the stand is shown in Fig. 1C and photographs in Figure 1A, 1B. The vibration generator, an electromagnetic actuator, is positioned on a stationary base. The principle of its operation is based on coil movement, which is generated by an alternating current flow. The design of the actuator is similar to that of a typical loudspeaker, with the main difference being that the moving parts are not a flexible membrane but a stiff plate.

The stiff plate of the actuator moves in a linear manner in relation to the stationary part. Fig. 1C depicts the displacement value as ‘x’. Between the actuator and the culture plate, a spacer has been mounted. The spacer is a rigid element made of polyethylene, placed to create distance from the cell culture actuator. This was done to eliminate the possible influence of the alternating magnetic field generated by the EM-actuator on the cell culture. The height of the spacer was about 10 cm. The strength of the magnetic field at this distance does not differ from the background.

The culture plate was attached to the top surface of the spacer in such a way to allow quick mounting. Such a method was dictated by the fact that the vibration stimulation was scheduled only for short periods of time each day. Movement of the culture plate was defined as a course of the sine function with a given value of frequency and amplitude of acceleration. A laser

displacement sensor (KEYENCE LK-G157) was used to measure the translation of the culture plate. The acceleration signal was calculated according to the following formula:

$$x = Asin(\omega t) \quad \rightarrow \quad \ddot{x} = -A\omega^2 sin(\omega t)$$

where $x$ – displacement, $\ddot{x}$ – acceleration, $A$ – amplitude of displacement, $\omega$ – frequency of vibrations ($\omega = 2\pi f$), $f$ – frequency, $t$ – time, $A\omega^2$ – amplitude of acceleration.

***Vibration loading protocol of hASCs culture***

The hASCs were seeded at a concentration of $1.5\times10^4$ on 24 - well plates. For each vibration model (25, 35 and 45Hz) separate dishes were used. Plates were placed securely onto the vibration device and subjected to 25, 35 and 45 Hz of sinusoidal vibrations at 0.3$g$ for 15 minutes once a day, for 14 consecutive days. Cells in the non-vibration group were placed on the same but stationary plate. After 15 min of vibration, the hASCs (both vibrated and non-vibrated groups) received fresh culture medium.

***Isolation of human adipose derived mesenchymal stem cells (hASCs)***

This study was approved by the local bioethics committee of Wroclaw Medical University, Poland (number KB-177/2014). Written informed consent was obtained from each patient prior to tissue collection during total hip arthroplasty. This study adhered to the Helsinki Declaration (1964) and its later amendments.

Subcutaneous adipose tissue was collected from 4 patients. From each patient we obtained 4 donor samples, representing of a total n=16. The average age of the patients was 69±1 years. Briefly, after collection, the tissue samples were placed in sterile Hank's Balanced Salt Solution (HBSS). The isolation procedure of adipose-derived mesenchymal stem cells was conducted under aseptic conditions and in accordance with previously described protocol [27, 28]. Samples

were washed with HBSS supplemented with a 1% antibiotic-antimicotic solution (penicillin/streptomycin/amphotericin b at a concentration of 0.017mol/l, 0.01mol/l and 0.0002mol/l respectively; Sigma Aldrich, cat no A5955) and then cut into small pieces using surgical scissors. Next, the samples were placed in a sterile centrifuge tube and digested with type I collagenase (1 mg/ml, Sigma Aldrich, cat no C5894). After 30 minutes incubation at 37°C, the tissue homogenate was centrifuged at 1200g for 10 minutes. The supernatant was removed and the cell pellet was resuspended in growth media. The cell suspension was then transferred to the cell culture flask.

***Immunophenotyping, Fluorescence-activated cell sorting (FACs) analysis, and multipotency test***

Cells were plated on 24-well culture plates suspended in 500 µl of standard medium at a concentration of 8 x $10^3$ cells per well. The presence of specific antigens for ASCs, i.e. integrin beta-1 (CD29), HCAM (CD44), 5'-nucleotidase (CD73) and endoglin (CD105) and leukocyte common antigen (CD45) was examined after one week of culture by means of primary antibodies (all from Sigma Aldrich). Negative staining of CD45 was used to exclude hematopoietic origin. After fixation, cells were permeabilized with 0,2% Tween 20 for 15 minutes and washed three times with HBSS. The solution of primary antibody and 4% FBS in PBS was applied to every well and incubated overnight at 4°C. Next, the cells were washed three times and secondary goat anti-rabbit conjugated with Atto 488 antibody was added to appropriate wells at concentration 1:150. After incubation at room temperature for 1.5 hours, the cells were washed again and photographed under a fluorescence microscope.

For the multipotency test, cells were cultured on chondrogenic and adipogenic media (STEMPRO® Chondrogenesis/Osteogenesis Differentiation Kit and STEMPRO® Adipogenesis Differentiation Kit, Life Technologies) for 14 days. The culture media was changed every second day.

After 3 passages, the ASCs were examined for surface protein molecule expression by flow cytometry. Cells were trypinized using a Trypsin-EDTA solution (TrypLE$^{TM}$, Life Technologies), centrifuged at 400 xg for 3 minutes, and then washed with PBS containing 2% FBS (fetal bovine serum) (Sigma Aldrich). A total of 5 x $10^5$ cells were labeled for 20 min (on ice and dark) with antibodies pre-conjugated with allophycocyanin (APC), peridinin chlorphyllprotein (PerCP), fluorescein isothiocyanate (FITC) or phycoerythrin (PE). The following CD surface markers were tested: CD34, CD45, CD105, CD90, CD73, CD44, CD29 and IgG1 as an isotype control antibody (BD Pharmingen). The samples were analyzed by a Becton Dickinson FACSCalibur flow cytometer. At least ten thousand events were acquired for each CD surface marker. The data was then analyzed using FlowJo X software (Treestar).

***Cell culture***

Throughout the experiment, isolated hASCs were cultured in aseptic and constant conditions in an incubator at 37°C, 5% $CO_2$ and 95% humidity. The cell population was plated in T-75 culture flasks for primary culture and was maintained in Dulbecco's Modified Eagle's Medium (DMEM) with nutrient F-12 Ham (Sigma Aldrich) supplemented with 10% FBS and 1% of antibiotic/antimicotic solution at a concentration of 0,017mol/l, 0,01mol/l and 0,0002mol/l respectively (Sigma Aldrich, cat no A5955). The culture medium was changed every second day. Human ASCs were passaged using Trypsin-EDTA solution (TrypLE$^{TM}$, Life Technologies) in

accordance with manufacturer's instruction after reaching about 80-90% confluence. Cells were passaged three times before use in experiments.

Isolated adipose-derived mesenchymal stem cells were divided into 2 groups. The first one was stimulated with chondrogenic medium and the second one with adipogenic medium. The differentiation processes of hASCs were performed using the STEMPRO® Chondrogenesis Differentiation Kit and STEMPRO® Adipogenesis Differentiation Kit (Life Technologies), respectively. The stimulation of cells was performed in accordance with the manufacturers' instruction.

The chondrogenic culture was maintained in two systems: 2D in 24-well plates for fluorescent, histochemical stainnings, rtPCR analysis and SEM, and 3D for ELISA tests and Focused Ion Beam Scanning Electron Microscope (FIB-SEM, Auriga Compact Crossbeam, Zeiss, Germany). For the 3D system, $2.5 \times 10^5$ hASCs were seeded into 15 ml polypropylene tubes and pelleted. The hASCs were cultured for 21 days as 3D pellets in induction medium STEMPRO® Chondrogenesis Differentiation Kit (Life Technologies). The experiment was repeated three times.

***Cell proliferation assay***

The cell proliferation factor (PF) was evaluated using the Almar Blue test (TOX-8, Sigma Aldrich) according to the manufacturer's instructions. The culture media was replaced with a medium containing 10% of resazurin-based dye and incubated for two hours. Afterwards, the supernatants were collected and subjected to absorbance measurement by means of spectrophotometer (SPECTRO StarNano, BMG Labtech) at 600 nm of wavelength, with a

distraction of 690 nm of background absorbance. The procedure was performed during the differentiation period at days 2, 5, 10, and 14.

A standard curve obtained during the experiment, allowed to estimate the amount of cells. The population doubling time (PDT) was assessed using an on-line calculator (http://www.doubling-time.com/compute.php).

***Examination of hASCs morphology***

Cell morphology, cellular composition, and culture growth pattern were analyzed using an inverted, fluorescence microscope (AxioObserverA1, Zeiss) and a scanning electron microscope (SEM; EVO LS15, Zeiss).

In order to begin observations, after the culture period, cells were fixed with 4% paraformaldehyde. After 15-minutes permeabilization with 0.2% Tween, cells were stained using atto-565-labeled phalloidin for 40 minutes to visualize actin filaments. After triple washing, diamidino-2-phenylindole (DAPI) staining was applied for 5 min to analyze the distribution of cell nuclei. All fluorescence staining was performed at room temperature in the dark. Additionally, Oil Red O staining for adipogenic cultures and Safranin-O staining for chondrogenic cultures were performed to observe fat droplets and chondrocytes, respectively. After fixation, adipogenic samples were treated with 60% isopropanol for 5 min, solution of Oil Red O stain for 5 min. Chondrogenic samples were treated with 1% acetic acid for 10 min and stained with Safranin-O for 5 minutes. Images were acquired using a Cannon PowerShot digital camera. To analyze detailed morphological features of the cells, especially fat droplets, and chondrogenic nodules, SEM was performed. After fixation, the cells were washed in distilled water and dehydrated in ethanol (concentrations from 50 to 100%, every 5 min). Thoroughly

dried cells were coated with gold (ScanCoat 6, Oxford), placed in a microscope chamber, and observed using the SE1 detector, at 10 kV of filament's tension. To observe morphological features and measure diameters of nodules Ion Beam Scanning Electron Microscope (FIB-SEM, Auriga Compact Crossbeam, Zeiss, Germany) obsrvations were performed. Analysis was performed using a focus ion beam detector at magnification of 200X.

***Quantitative, Collagen type 1 and 2 (Col-1, Col-2) Bone Morphogenetic Protein 2 (BMP-2) assay***

In order to evaluate the chondrogenic differentiation efficiency on the protein level, the concentration of chondrogenesis-specific markers was investigated. The total concentration of proteins from pellet cultures was determined with enzyme-linked immunosorbent assay (ELISA). For the analysis, supernatants were collected on the last day of the experiment. Chondrogenic media was subjected to a BMP-2 ELISA assay (Bone Morphogenic Protein 2 Quantikine ELISA Kit, R&D Systems), and a Col-1 and a Col-2 ELISA assay (Human Collagen alpha-1(I) and (II) chain ELISA Kit, EIAab). All steps of each ELISA tests were performed in accordance with the manufacturer's protocol. Each sample was prepared in duplicate. Spectrofotometric determination was performed using a microplate reader (Spectrostar Nano, BMG Labtech) at a wavelength equal to 450 nm and with the correction wavelength of 540 nm. The concentration of proteins was presented as a ratio of protein weight and supernatant volume (w/v).

**Quantitative Real-Time Reverse Transcription Polymerase Chain Reaction (qRT-PCR)** In order to analyze gene expression, cells after stimulation were rinsed with HBSS and were homogenized with 0.5 ml of TRI Reagent (Sigma Aldrich) directly in the culture well. The total

RNA was isolated using a phenol-chloroform method as previously described [29]. After isolation, total RNA was diluted in DEPC-treated water. The concentration and purity of RNA preparations was determined by absorbance measured at 260 nm with a nanospectrophotometer (VPA biowave II). Preparation of DNA-free RNA was performed using DNase I RNase-free kit (Thermo Scientific). For each reaction, 100 ng of total RNA was used. Transcription of gDNA-free total RNA to a complementary DNA (cDNA) was reverse transcribed using Moloney Murine Leukemia Virus Reverse Transcriptase (M-MLV RT) and oligo(dT)15 primers (Novazym). RNA purification and cDNA transcription was performed according to manufacturers' instructions. Quantitative Real-Time polymerase chain reaction (qRT-PCR) was performed using 5 µl of cDNA in total volume of 20 µl by means of SensiFast SYBR & Fluorescein Kit (Bioline). The reaction was performed at a 500 nM final concentration of primers. The primer sequences used are presented in Table 1. qRT-PCR was performed as described previously [30]. Expression levels of all analyzed genes were normalized for the expression level of glyceraldehyde-3-phosphate dehydrogenase (GAPDH), a housekeeping gene.

***Statistical Analysis***

All experiments were performed with n = 3 or more. Statistical analysis was performed using GraphPad Prism 5 software. The statistical significance of results was calculated using the one-way analysis of variance (ANOVA) with post-hoc Dunnett's test by means. A P-value of less than 0.05 was considered statistically significant.

## Results

### *hASCs - FACs analysis, immunophenotyping and multipotency test*

Flow cytometry analysis revealed that hASCs showed positive labeling for CD29, CD44, CD73, CD105, and CD90 (Fig. 2B). The investigated cells were negatively labeled for two hematopoietic markers: CD34 and CD45 (Fig. 2B). Additionally, immunohistochemical staining confirmed the presence of mesenchymal markers (CD29, CD44, CD73, CD105) and excluded hematopoietic origin (CD45) (Fig. 2A).

Moreover, the multipotent character of hASC's was confirmed by abundant osteogenic and adipogenic differentiation. In contrast to cells cultured under control conditions, the presence of osteo nodules, was observed in hASCs cultivated under osteogenic conditions (Fig. 2C). Moreover, mineral calcium deposits visualized by Alizarin Red staining were clearly detected after 3 weeks of osteogenic differentiation. After 2 weeks of culture with an adipogenic inducing media, hASCs developed Oil Red O positive lipid droplets (Fig. 2C), whereas control cultures grown in standard media failed to produce similar results (Fig. 2C).

### *Proliferation rate (PF) and population doubling time (PDT) of 3D chondroblasts originated from chondro induced hASCs.*

The proliferative activity, as well as the PDT, were analyzed during the 14 days of hASCs culturing in chondrogenic induction medium exposed to vibration frequencies of 25, 35 and 45Hz and in non-vibration control conditions. The obtained data showed that all investigated vibration frequencies significantly influenced the proliferative potential, as well as the PDT, of chondroblasts originated from hASCs (Fig. 3A, B). The percentage of Alamar Blue reduction decreased proportionally with cell count and activity.

297 Cells cultured under 25 Hz frequency reached the highest PF after 2 days of incubation and then
298 declined, but on the 10th day of culture reached higher PF and declined again till the 14th day.
299 Moreover, we noticed the longest PDT (277±25 hours) when cells were stimulated with a 25Hz
300 frequency. The cells exposed to 35Hz vibrations had a higher PF than control cultures at all
301 investigated time points (Fig. 3A). During the analysis, hASCs after chondrogenic differentiation
302 using 25Hz vibrations resulted in the lowest proliferation potential, as well as longest PDT, when
303 compared to the other investigated groups.

304 ***The morphology of chondroblasts originated from hASCs***

305 After 14 days, formation of chondroblast-specific nodules could be clearly observed (Fig. 4A-P,
306 Fig. 5A-D, Panel B) and showed a strong orange signal after Safranin O staining (Fig. 4I-L).
307 Characteristic chondrocyte-like cells were observed in all of the investigated cultures, however,
308 the cells cultured under the influence of 35Hz vibrations more efficiently induced
309 chondrodifferentiation (Fig. 4N). In these samples, nodules had the largest size (Fig. 6A) as well
310 as exhibited the highest absorption of Safranin O (Fig. 6B). Cells cultured under 25Hz vibrations
311 absorbed less Safranin O dye and formed nodules with a significantly smaller diameter than
312 samples cultured with 35 Hz vibrations (Fig. 6A, B). Chondroinduction of cells treated with
313 45Hz were comparable to the control group. Although chondro-nodules had similar diameters,
314 the absorption of Safranin O by cells cultured with 45 Hz frequencies was significantly higher
315 (Fig. 6A, B).

316 ***Quantitative Collagen 1 and 2 (Col-1, Col-2) and Bone Morphogenetic Protein 2 (BMP-2)***
317 ***assay and chondrogenic gene expression analysis (SOX-9, Col-X, Col-II, Runx, Col-I, ACAN)***

318 The performed analysis showed an increase in collagen type 2 concentration in comparison to the
319 amount of collagen type I in all groups where vibrations were applied (Fig. 5A, B, Panel A).
320 These results were additionally confirmed by positive chondrogenic differentiation of hASCs.

321 The highest difference between collagen type II and type I was observed in the cultures
322 stimulated with 25 and 35 Hz vibrations, and in the control culture. The lowest concentration of
323 collagen type II with respect to collagen type I was observed when 45 Hz frequency vibrations
324 were applied (Fig. 5A, B, Panel A). Cells treated with 35Hz frequency vibrations tended to
325 secrete significantly higher amounts of BMP-2 in comparison to the other groups (Fig. 5C, Panel
326 A). Exposure to the 25Hz stimulation model resulted in secretion of lower a concentration of
327 BMP-2 in comparison to the 35Hz, however significantly higher when compared to the 45Hz
328 frequencies, as well as to the control culture.

329 The quantitative evaluation of the concentration of collagen type I and type II was additionally
330 confirmed by gene expression analysis (Fig. 4C, E, Panel A). The highest activity of collagen
331 type II and its predominance over expression of collagen type I was observed in cells treated
332 with 35Hz vibrations. Similarly to the quantitative evaluation, exposure to 25Hz vibrations
333 resulted in lower expression of Collagen type II when compared to the 35Hz vibrations model.
334 The gene expression of SOX-9 and Col-X, the master transcription factors of chondrogenesis,
335 gradually increased in 35 Hz treated cells compared to control group (Fig. 4A, B, Panel A).
336 Aggrecan (ACAN) and RUNX2, another chondrogenic markers, significantly increased after 25
337 Hz treatment (Fig. 4D, F, Panel A).

***Analysis of integrin expression in response to vibration stimulation***

In order to sense and translate the applied external mechanical signals, cells express mechanoreceptors on their surface, such as integrins. In our study, we analyzed the expression changes of four alpha (α3, α 4, α 5 and αV) and three beta (β1, β3 and β5) integrin subunits (Fig. 7). qPCR analysis demonstrated a slight increase of integrin α3, α4, β1 and β3 subunit expression after 25 Hz stimulation in comparison to control (0 Hz). We also found that when cells were stimulated with 35 Hz vibrations, hASCs significantly upregulated integrin α3, α4, β1 and β3 subunit. Interestingly, after 35 Hz stimulation, the highest increase in expression of the β3 intergrin was observed. With respect to integrin subunits α5, αV, and β5, expression levels were similar between to stimulated groups, however down-regulated as compared to control.

***Proliferation factor and population doubling time of human adipocytes originated from adipo induced hASCs.***

The proliferation factor and PDT were determined in the various groups after 14 days of adipogenic induction. The stimulated cultures were characterized by an irregular proliferation rate (Fig. 8A). Stimulation with a 25 Hz frequency resulted in a significant increase of PF when compared with the other groups. The highest PF was on day 5, and from that point on a decreasing trend was observed (Fig. 8A). The 25Hz frequency group also has the shortest PDT in comparison to other experimental groups (Fig. 8B).

In the 35Hz and 45 Hz treatment groups, proliferation remained significantly decreased at days 2, 5 and 10 of culture in comparison to the control and 25 Hz group, although this difference was not as pronounced as that on day 14. These results were also reflected in the PDT calculations - the 35 Hz and 45 Hz cultures had longer time to achieving PDT (Fig. 8B).

360 ***Morphology of ASCs after adipogenic differentiation***

361 Microscopic analysis of adipocytes that originated from hASCs revealed that the 25 Hz
362 vibrations mostly enhanced the adipogenic differentiation in comparison to the other groups (Fig.
363 9I, Panel B). The findings from gene expression analysis showed noticeable increase
364 of PPAR-γ and adiponectin (ADIQ) (Fig. 9A, B, Panel A) in 25 and 35 Hz stimulated groups
365 compared to control. However, qRT-PCR findings also showed similar gene expression of leptin
366 (LEP) (Fig. 9C, Panel A). The adipocytes derived from 25 Hz stimulated group were highly
367 abundant with large lipid vacuoles, positively stained by Oil Red O staining, and absorbed the
368 highest percentage of dye (Fig. 10A). The smallest adipocyte diameter was observed in the
369 control group (ranges between 60 and 92 um), while adipocytes treated with 35Hz were
370 characterized by the highest average size (ranges between 90 and 119 um) (Fig. 10B).
371
372

## Discussion

Cartilage defects, especially in cases of osteoarthritis, have a serious impact on the patient's quality-of-life and functionality. The increasing prevalence of degenerative joint diseases is explained by the increasing life expectancy of the general population [31]. Tissue-engineering approaches including the application of externally applied signals such as stimulation with electric currents [32, 33], laser [34], or ultrasound vibration [35, 36], are promising tools for overcoming this problem. However, these methods also have several shortcomings, such as emission of high temperature or generation of rarefactional pressure, which may lead to mild heating, coagulative necrosis, tissue vaporization or inducing pulsation of pre-existing gas bodies [37].

Even more promising is the combination of MSCs therapy with innovative devices that are able to induce particular external signals, which enhance the regeneration of injured tissues. Since stem cells viability, proliferation status, and differentiation potential are widely connected with their regenerative potential [38, 39], searching for external stimulating factors that may enhance the mentioned MSCs features, before clinical application seems to be a crucial factor, when MSCs for cartilage regeneration purposes are considered. Furthermore, effective external stimulation may help overcome the age-related decrease in chondrogenic differentiation potential of hASCs that currently poses a limitation to their clinical application in cell-based therapies [12]. Therefore, in the current study, we hypothesized that LMLF may enhance the chondrogenic differentiation potential of hASCs and simultaneously alter the differentiation toward fat tissue.

We found that when the PF of hASCs cultured in chondrogenic conditioned medium is considered, both the 25 Hz and the 35 Hz vibration frequencies reduce the PF of hASCs. Additionally, the PDT reached the highest level in cells treated with 25 Hz, which strongly

correlates with the obtained PF factor. As recently reported, the PDT of MSCs directly correlates with their replicative senescence, which is linked to the decrease in the size of cell aggregation [40]. In each experimental group, the PDT was higher in comparison with other studies [41]. This may be due to the fact that cells were rapidly differentiated into osteoblasts or adipocytes, and that their proliferation activity was significantly reduced. Sepúlveda et al. [42] reported that cell senescence abrogates the therapeutic potential of human mesenchymal stem cells in a lethal endotoxemia model. Therefore, searching for methods that might improve the PDT level seems to be crucial in the context of clinical application of MSCs. Interestingly, although hASCs treated with 35 Hz had low PF and long PDT, they also developed the largest chondro nodules. Furthermore, the highest concentration of absorbed Safranin O staining was observed in nodules originating from cells treated with 35 Hz vibration. This likely demonstrates that 35 Hz vibrations induce the highest synthesis of glycosaminoglycans (GAG), and thus indicates that the chondrogenic process is highly efficient.

The GAGs have an unquestionable influence on biomechanical properties of cartilage. They serve as an important component of extracellular matrix (ECM), which directly affects the integrity of cartilage. Our data demonstrates that the 35 Hz vibration model could be applied to stimulate chondrocytes, which originated from hASCs to produce ECM of high biomechanical properties. The most extensive morphometrical properties, i.e. length and height of single nodules, were observed in chondroblasts that were treated with the 35Hz vibrations protocol. Slightly weaker chondro nodule development, as well as cytoskeleton formation, was observed in the culture treated with 25Hz vibrations in comparison to the others, as well as to the control group.

In order to determine which of the investigated frequencies has a more significant impact on the process of chondrogenesis, we applied quantitative ELISA in order to evaluate the concentration of BMP-2 and the relationship between collagen type I and II in the culture medium. We found the highest concentrations of BMP-2, as well as collagen type II, in the culture treated with 35 Hz. However, 25 Hz vibrations caused an increase in synthesis, albeit slightly smaller amounts of investigated proteins. Our obtained results stand in good agreement with the findings of van Cashion et al. [43], who reported that low frequency vibrations can induce secretion of BMP-2 in human umbilical cord derived MSCs. It is worth noting that both the 25 Hz and 35 Hz vibration stimulated chondrocytes originating from hASCs had elevated synthesis of type II rather than type I collagen. It is well known that elasticity of articular cartilage is dependent on the proper relationship between synthesis and secretion of collagen types I and II. Simultaneously, we observed, that 35Hz vibration stimuli caused up-regulation of sex-determining region Y protein (SRY)-box 9 (SOX9) that is the primary regulator of chondrogenic differentiation on an in vitro as well as an in vivo level. The observed up-regulation of Sox-9, strongly corresponded with elevated expression of collagen type II, which is to be expected as Sox-9 directly regulates expression of collagen gene (COLL II) in chondrogenic progenitor cells, as well as chondrocytes [44, 45]. Moreover, SOX9 determines functions of RUNX2 and exerts a dominant function over RUNX2 in mesenchymal precursors. In this study, we confirmed this effect; gene expression of SOX9 and RUNX2 are overlapped and enhanced in cells treated with vibrations.

The positive effect of LFLM on the functional chondrogenic differentiation process might be explained by up-regulation of the integrin family. Here, we found that both frequencies i.e. 25 and 35 Hz, affect up-regulation of integrin α3, α4, β1 and β3 subunits on the mRNA level, although statistical significance was observed only in 35Hz stimulated cells. Furthermore, β1

integrin has been shown to play a crucial role in attachment and survival of MSCs during the chondrogenesis process. Form a tissue engineering point of view, the obtained data seems to be promising when application of the discussed "vibration device" in pre-clinical culture of MSCs is considered [46]. Furthermore, we observed that LFLM, in general, significantly down regulates integrin α5β5 expression. These obtained results shed a promising light for LFLM application in MSCs chondrogenic differentiation, since down-regulation of integrin α5β5, has been shown to protect stromal cells during differentiation from undergoing pre-hypertrophic chondrocytes [47]. Moreover, we observed down-regulation of α5 integrins of MSCs stimulated with all tested frequencies. Thus our results stand in good agreement with Martino and colleagues (2008), that showed involvement of α5 integrins more in osteogenic rather than chondrogenic differentiation process [48].

Finally, the effect of vibration loading with particular frequencies on the adipogenic differentiation potential of hASCs was investigated. We found that among all tested frequencies, 35 Hz significantly inhibited adipogenesis in hASCs. The obtained results stand in good agreement with the findings by Oh at al. [49] who reported that 20 and 30 Hz sub-sonic vibrations inhibited the proliferation of 3T3-L1 preadipocytes, Additionally, we observed the smallest absorption of Oil red O staining when cells were treated with 35 Hz vibration, However we observed increased number of lipid droplets in 25 Hz vibration group, but the observed changes were only on a morphological level. In adipogenic gene expression level of we did not observed significant changes between 25 Hz and other investigated groups.

## Conclusions

In conclusion, the vibration-loading device designed for the purpose of this study successfully generated controlled vibrational forces to hASCs cultured on 24-well, as well as 3D pelleted cells model. Our results indicate that LFLM vibrations differently act on both chondrogenic, as well as adipogenic potential of hASCs. The most important finding of this study suggests that 35 Hz frequency vibrations enhance chondrogenic potential of hASCs with simultaneous inhibition of hASCs differentiation toward adipocytes. Finally, we conclude that mechanical signals, especially 35 Hz frequency vibrations might be potentially used in construction of therapeutic devices which may prove useful in the field of articular degenerative diseases treatment.

## Acknowledgments

We thank Marta Jeleń for assistance during in vitro work and cell vibration generator prototype preparation.

## Funding Statement

The research was supported by Wroclaw Research Centre EIT + under the project 'Biotechnologies and advanced medical technologies'—BioMed (POIG.01.01.02-02-003/08) financed from the European Regional Development Fund (Operational Programmed Innovative Economy, 1.1.2.). Krzysztof A. Tomaszewski was supported by the Foundation for Polish Science (FNP).

## Disclosures

The authors declare that there is no conflict of interests regarding the publication of this paper.

## References


1. Chung C, and Burdick JA (2008). Engineering cartilage tissue. Advanced drug delivery reviews, 60(2), 243-262.
2. Lin J, Zhang W, Jones A and Doherty M (2004). Efficacy of topical non-steroidal anti-inflammatory drugs in the treatment of osteoarthritis: meta-analysis of randomised controlled trials. bmj, 329(7461), 324.
3. Iyer SS, Rojas M: Anti-inflammatory effects of mesenchymal stem cells: novel concept for future therapies. Expert Opin. Biol. Ther. 2008, 8(5): 569-581.
4. Zuk PA, Zhu M, Mizuno H, Huang J, Futrell JW, Katz AJ, Benhaim P, Lorenz HP, Hedrick MH. (2001) Multilineage cells from human adipose tissue: implications for cell-based therapies. Tissue Eng. 7, 211–228.
5. Baer PC, Geiger H: Adipose-derived mesenchymal stromal/stem cells: tissue localization, characterization, and heterogeneity. Stem cells 2012, doi:10.1155/2012/812693
6. Collino F, Deregibus MC, Bruno S, Sterpone L, Aghemo G, Viltono L, Camussi G (2010) Microvesicles derived from adult human bone marrow and tissue specific mesenchymal stem cells shuttle selected pattern of miRNAs. PloS one, 5(7), e11803.
7. Tetta C, Consiglio AL, Bruno S, Tetta E, Gatti E, Dobreva M, Cremonesi F, Camussi G (2012) The role of microvesicles derived from mesenchymal stem cells in tissue regeneration; a dream for tendon repair? Muscles Ligaments Tendons J. 2(3): 212–221.
8. Marycz K, Grzesiak J, Wrzeszcz K, Golonka P. (2012) Adipose stem cell combined with plasma-based implant bone tissue differentiation in vitro and in a horse with a phalanx digitalis distalis fracture: a case report. Veterinarni Medicina 57(11): 610–617; 2012.

9. Marycz K, Toker NY, Grzesiak J, Wrzeszcz K, Golonka P. (2012) The therapeutic effect of autogenic adipose derived stem cells combined with autogenic platelet rich plasma in tendons disorders hi horses in vitro and in vivo research. Journal of Animal and Veterinary Advances 11(23): 4324–4331; 2012.

10. Brittberg M, Lindahl A, Nilsson A, et al. Treatment of deep cartilage defects in the knee with autologous chondrocyte transplantation. N Engl J Med 1994; 331: 889–895.

11. Nicpoń J, Marycz K, Grzesiak J, Śmieszek A, Toker ZY (2014). The advantages of autologus adipose derived mesenchymal stem cells (AdMSCs) over the non-steroidal anti-inflammatory drugs (NSAIDs) application for degenerative elbow joint disease treatment in dogs-Twelve cases. Kafkas Univ Vet Fak Derg, 20(3), 345-350.

12. Choudhery MS, Badowski M, Muise A, Pierce J, Harris DT. Donor age negatively impacts adipose tissue-derived mesenchymal stem cell expansion and differentiation. J Transl Med. 2014;12:8.

13. Marędziak M, Marycz K, Śmieszek A, Lewandowski D, Nezir Yaşar Toker (2014) The influence of static magnetic fields on canine and equine mesenchymal stem cells derived from adipose tissue. In Vitro Cell.Dev.Biol. – Animal, 50:562–571.

14. Hammerick KE, James AW, Huang Z, Prinz FB, Longaker MT. (2009) Pulsed direct current electric fields enhance osteogenesis in adipose-derived stromal cells. Tissue Engineering Part A, 16(3), 917-931.

15. Simmons CA, Matlis S, Thornton AJ, Chen S, Wang CY, Mooney DJ. (2003). Cyclic strain enhances matrix mineralization by adult human mesenchymal stem cells via the extracellular signal-regulated kinase (ERK1/2) signaling pathway. Journal of biomechanics, 36(8), 1087-1096.

16. Nikander, R. et al. (2009) Targeted exercises against hip fragility. Osteoporos. Int. 20, 1321–1328.

17. Tirkkonen L, Halonen H, Hyttinen J, Kuokkanen H, Sievänen H, Koivisto AM, Haimi S (2011). The effects of vibration loading on adipose stem cell number, viability and differentiation towards bone-forming cells. Journal of The Royal Society Interface, 8(65), 1736-1747.

18. Luu YK, Capilla E, Rosen CJ, Gilsanz V, Pessin JE, Judex S, Rubin CT. (2009) Mechanical stimulation of mesenchymal stem cell proliferation and differentiation promotes osteogenesis while preventing dietary-induced obesity. J. Bone Miner. Res. 24, 50–61.

19. Goessler UR, Bugert P, Bieback K, et al. In vitro analysis of integrin expression in stem cells from bone marrow and cord blood during chondrogenic differentiation. J Cell Mol Med. 2009;13(6):1175-84.

20. Hering TM. Regulation of chondrocyte gene expression. Front Biosci. 1999;4:D743-61.

21. Hynes RO. Integrins: versatility, modulation, and signaling in cell adhesion. Cell. 1992;69(1):11-25.

22. Giancotti FG, Ruoslahti E. Integrin signaling. Science. 1999;285(5430):1028-32.

23. Albelda SM, Buck CA. Integrins and other cell adhesion molecules. FASEB J. 1990;4(11):2868-80.

24. Salter DM, Hughes DE, Simpson R, Gardner DL. Integrin expression by human articular chondrocytes. Br J Rheumatol. 1992;31(4):231-4.

25. Lee J BC, W, Qi WN, Scully SP. The involvement of beta1 integrin in the modulation by collagen of chondrocyte-response to transforming growth factor-beta1. J Orthop Res. 2002;20(1):66-75.

555 26. Rubin C, Judex S, Qin YX. (2006) Low-level mechanical signals and their potential as a non-
556 pharmacological intervention for osteoporosis. Age Ageing 35, 32.
557 27. Grzesiak J, Marycz K, Czogala J, Wrzeszcz K, Nicpon J (2011) Comparison of behavior,
558 morphology and morphometry of equine and canine adipose derived mesenchymal stem cells
559 in culture. Int J Morphol 29: 1012–1017.
560 28. Marycz K, Smieszek A, Grzesiak J, Donesz-Sikorska A, Krzak-Ros J (2013) Application of
561 bone marrow and adipose-derived mesenchymal stem cells for testing the biocompatibility of
562 metal-based biomaterials functionalized with ascorbic acid. Biomed Mater 8: 065004.
563 29. Chomczynski P, Sacchi N (1987) Single-step method for RNA isolation by acid guanidinium
564 thiocyanate-phenol-chloroform extraction. Anal Biochem 162: 156-159.
565 30. Kim HJ, Im GI. The effects of ERK1/2 inhibitor on the chondrogenesis of bone marrow- and
566 adipose tissue-derived multipotent mesenchymal stromal cells. Tissue Eng Part A
567 2010;16(3):851e60.
568 31. Raeissadat S, Rayegani S, Babaee M, Ghorbani E (2013): The Effect of Platelet-Rich Plasma
569 on Pain, Function, and Quality of Life of Patients with Knee Osteoarthritis, Pain Res Treat.
570 2013; 2013: 165967.
571 32. Ciombor DM, Aaron RK. (2005) The role of electrical stimulation in bone repair. Foot Ankle
572 Clin; 10:579–593, vii.
573 33. Foley KT, Mroz TE, Arnold PM, Chandler HC Jr, Dixon RA, Girasole GJ, Renkens KL Jr,
574 Riew KD, Sasso RC, Smith RC, Tung H, Wecht DA, Whiting DM. Randomized,
575 prospective, and controlled clinical trial of pulsed electromagnetic field stimulation for
576 cervical fusion. Spine J. 2008;8:436–442.

577 34. Miloro M, Miller JJ, Stoner JA. Low-level laser effect on mandibular distraction
578 osteogenesis. J Oral Maxillofac Surg. 2007;65:168–176.
579 35. El-Mowafi H, Mohsen M. The effect of low-intensity pulsed ultrasound on callus maturation
580 in tibial distraction osteogenesis. Int Orthop. 2005;29:121–124.
581 36. Taylor KF, Rafiee B, Tis JE, Inoue N. (2007) Low-intensity pulsed ultrasound does not
582 enhance distraction callus in a rabbit model. Clin Orthop Relat Res;459:237–245.
583 37. Miller D, Smith N, Bailey M, Czarnota G, Hynynen K, Makin I, and American Institute of
584 Ultrasound in Medicine Bioeffects Committee (2012): Overview of Therapeutic Ultrasound
585 Applications and Safety Considerations, J Ultrasound Med.; 31(4): 623–634.
586 38. Krampera M, Pasini A, Pizzolo G, Cosmi L, Romagnani S, Annunziato F (2006):
587 Regenerative and immunomodulatory potential of mesenchymal stem cells; Current Opinion
588 in Pharmacology, Volume 6, Issue 4, August 2006, Pages 435–441.
589 39. Mishra A, Tummala P, King A, Lee B, Kraus M, Tse V, Jacobs CR (2009): Buffered
590 Platelet-Rich Plasma Enhances Mesenchymal Stem Cell Proliferation and Chondrogenic
591 Differentiation Tissue Engineering Part C: Methods, Vol. 15, No. 3: 431-435
592 40. Yoon IS, Chung CW, Sung JH, Cho HJ, Kim JS, Shim WS, Shim CK, Chung SJ, Kim DD.
593 Proliferation and chondrogenic differentiation of human adipose-derived mesenchymal stem
594 cells in porous hyaluronic acid scaffold. J Biosci Bioeng. 2011 Oct;112(4):402-8.
595 41. Hass, R., Kasper, C., Bohm, S., & Jacobs, R. (2011). Different populations and sources of
596 human mesenchymal stem cells (MSC): a comparison of adult and neonatal tissue-derived
597 MSC. Cell Commun Signal, 9(1), 12.

598 42. Sepúlveda JC, Tomé M, Fernández ME, Delgado M, Campisi J, Bernad A, González MA
599 (2014). Cell senescence abrogates the therapeutic potential of human mesenchymal stem
600 cells in the lethal endotoxemia model. Stem Cells.
601 43. Cashion A, Caballero M, Halevi A, Pappa A, Dennis RG, van Aalst JA (2014):
602 Programmable Mechanobioreactor for Exploration of the Effects of Periodic Vibratory
603 Stimulus on Mesenchymal Stem Cell Differentiation, BioResearch Open Access, Volume 3,
604 Number 1.
605 44. Akiyama H. Control of chondrogenesis by the transcription factor Sox9. Mod. Rheumatol.
606 2008;18, 213–219
607 45. Bell DM, Leung KK, Wheatley SC, et al. SOX9 directly regulates the type-II collagen gene.
608 Nat Genet. 1997;16(2):174-8.
609 46. Docheva D, Haasters F, Schemer M. Mesenchymal Stem Cells and Their Cell Surface
610 Receptors. Current Rheumatology Reviews. 2008;4(3):000-000.
611 47. Han Q, Fan L, Heng, GE Xizang. Apoptosis and Metabolism of Mesenchymal Stem Cells
612 during Chondrogenic Differentiation In Vitro. Int J Tissue Reg. 2013;4(3):61-64.
613 48. Martino MM, Mochizuki M, Rothenfluh DA, Rempel SA, Hubbell JA, Barker TH.
614 Controlling integrin specificity and stem cell differentiation in 2D and 3D environments
615 through regulation of fibronectin domain stability. Biomaterials. 2009;30(6):1089-97.
616 49. Oh ES, Seo YK, Yoon HH, Cho H, Yoon MY, Park JK (2011): Effects of sub-sonic vibration
617 on the proliferation and maturation of 3T3-L1 cells. Life Sci, Jan 17;88(3-4):169-77

618

619

620

621 **Tables:**

| Gene name | Primer sequentions | Ann. T, °C | Accession number |
|---|---|---|---|
| **GAPDH** | Forward 5'- GTCAGTGGTGGACCTGACCT -3'<br>Reverse 5'- CACCACCCTGTTGCTGTAGC -3' | 60 | NM_002046 |
| **Collagen type I (COL1A1)** | Forward 5'- GTGATGCTGGTCCTGTTGGT -3'<br>Reverse 5'- CACCATCGTGAGCCTTCTCT -3' | 60 | NM_000088.3 |
| **Collagen type II (COL2A1)** | Forward 5'- GACAATCTGGCTCCCAAC -3'<br>Reverse 5'- ACAGTCTTGCCCCACTTAC -3' | 60 | NM_001844.4 |
| **Aggrecan (ACAN)** | Forward 5'- GCCTACGAAGCAGGCTATGA -3'<br>Reverse 5'- GCACGCCATAGGTCCTGA -3' | 60 | NM_013227.3 |
| **SOX-9** | Forward 5'-AGCGAACGCACATCAAGAC-3'<br>Reverse 5'- GCTGTAGTGTGGGAGGTTGAA-3' | 65 | NM_000346 |
| **RUNX-2** | Forward 5'- GTGATAAATTCAGAAGGGAGG-3'<br>Reverse 5'- CTTTTGCTAATGCTTCGTGT-3' | 65 | NM_001024630 |
| **Collagen type X (Col-X)** | Forward 5'-CAGTCATGCCTGAGGGTTTT-3'<br>Reverse 5'-GGGTCATAATGCTGTTGCCT-3' | 65 | NM_000493 |
| **Adiponectin (ADIQ)** | Forward 5'-AGGGTGAGAAAGGAGATCC-3'<br>Reverse 5'- GGCATGTTGGGGATAGTAA-3' | 60 | XM_011513324.1 |
| **Leptin (LEP)** | Forward 5'- ATGACACCAAAACCCTCATCAA-3'<br>Reverse 5'- GAAGTCCAAACCGGTGACTTT-3' | 60 | XM_005250340.3 |
| **PPAR-gamma** | Forward 5'- ATGACACCAAAACCCTCATCAA- 3'<br>Reverse 5'- GAGCGGGTGAAGACTCATGTCTGTC-3' | 60 | AB565476.1 |
| **Integrin α3** | Forward 5´-ATCTTGAGAGCCACAGTCA-3´<br>Reverse 5´-cTGGGTCCTTCTTTCTAGTTC-3´ | 52 | (NM_002204) |
| **Integrin α4** | Forward 5´-AATGGATGAGACTTCAGCACT-3´<br>Reverse 5´-CTCTTCTGTTTTCTTCTTGTAGG-3´ | 58 | (NM_000885) |
| **Integrin α5** | Forward 5´-ACTAGGAAATCCATTCACAGTTC-3´<br>Reverse 5´-GCATAGTTAGTGTTCTTTGTTGG-3´ | 52 | (NM_002205) |

| | | | |
|---|---|---|---|
| **Integrin αv** | Forward 5′-GGAGCACATTTAGTTGAGGTAT -3′<br>Reverse 5′-ACTGTTGCTAGGTGGTAAAACT-3′ | 56 | (NM_002210) |
| **Integrin β3** | Forward 5′-CTGCTGTAGACATTTGCTATGA-3′<br>Reverse 5′-GCCAAGAGGTAGAAGGTAAATA-3′ | 52 | (NM_000212) |
| **Integrin β5** | Forward 5′-CTGTGGACTGATGTTTCCTT-3′<br>Reverse 5′-GTATGCTGGTTTTACAGACTCC-3′ | 54 | (NM_002213) |
| **Integrin β5** | Forward 5′- GAAGGGTTGCCCTCCAGA -3’ Reverse 5′- GCTTGAGCTTCTCTGCTGTT-3’ | 60 | NM_002211.3 |

622 **Table 1**. Sequences of qPCR primers used for the amplification of human mRNA to chondrogenic genes.

623

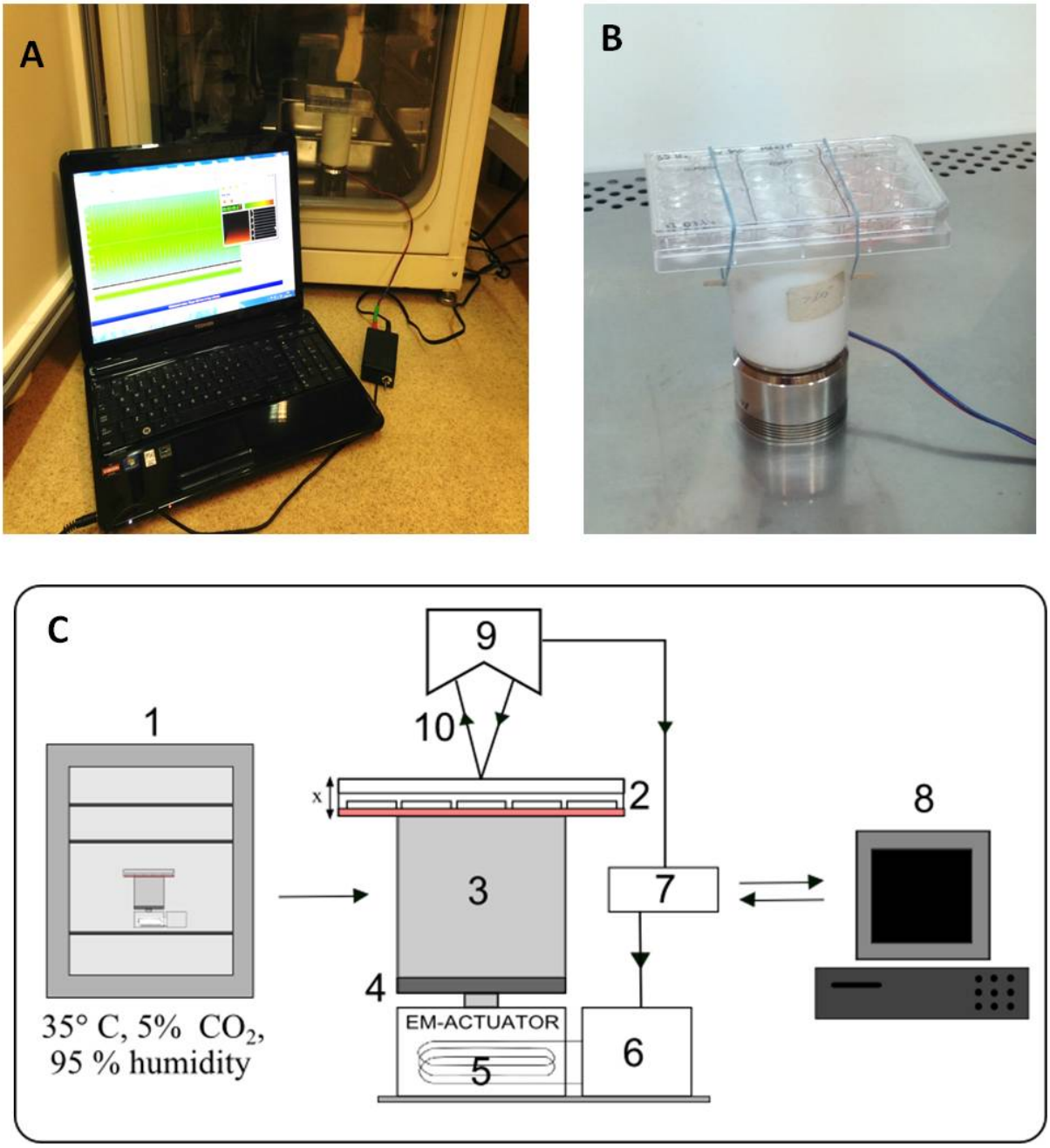


624

625 **Figure 1.** Cell vibration generator prototype. Acutator with cell culture plate connected with PC software, put inside
626 a CO2 incubator (A). Cell culture plate attatched to the spacer under electro-magnetic acutator (B). Connection
627 diagram and flow of signals during vibration stimulation. The electromagnetic actuator was supplied directly by the
628 amplifier. The displacement signal waveform was generated in the computer software and sent through a digital-to-
629 analog converter to the amplifier. 1 – incubator, 2 - 24-well culture plate, 3 – spacer, 4 – stiff movable plate, 5 –
630 electro-magnetic actuator (EM-ACTUATOR) with coil inside, 6 – signal amplifier, 7 – measuring card with A/C

and C/A converters, 8 – PC and software, 9 – laser displacement sensor head, 10 – laser beam. x shows the movement direction of the culture plate (C)

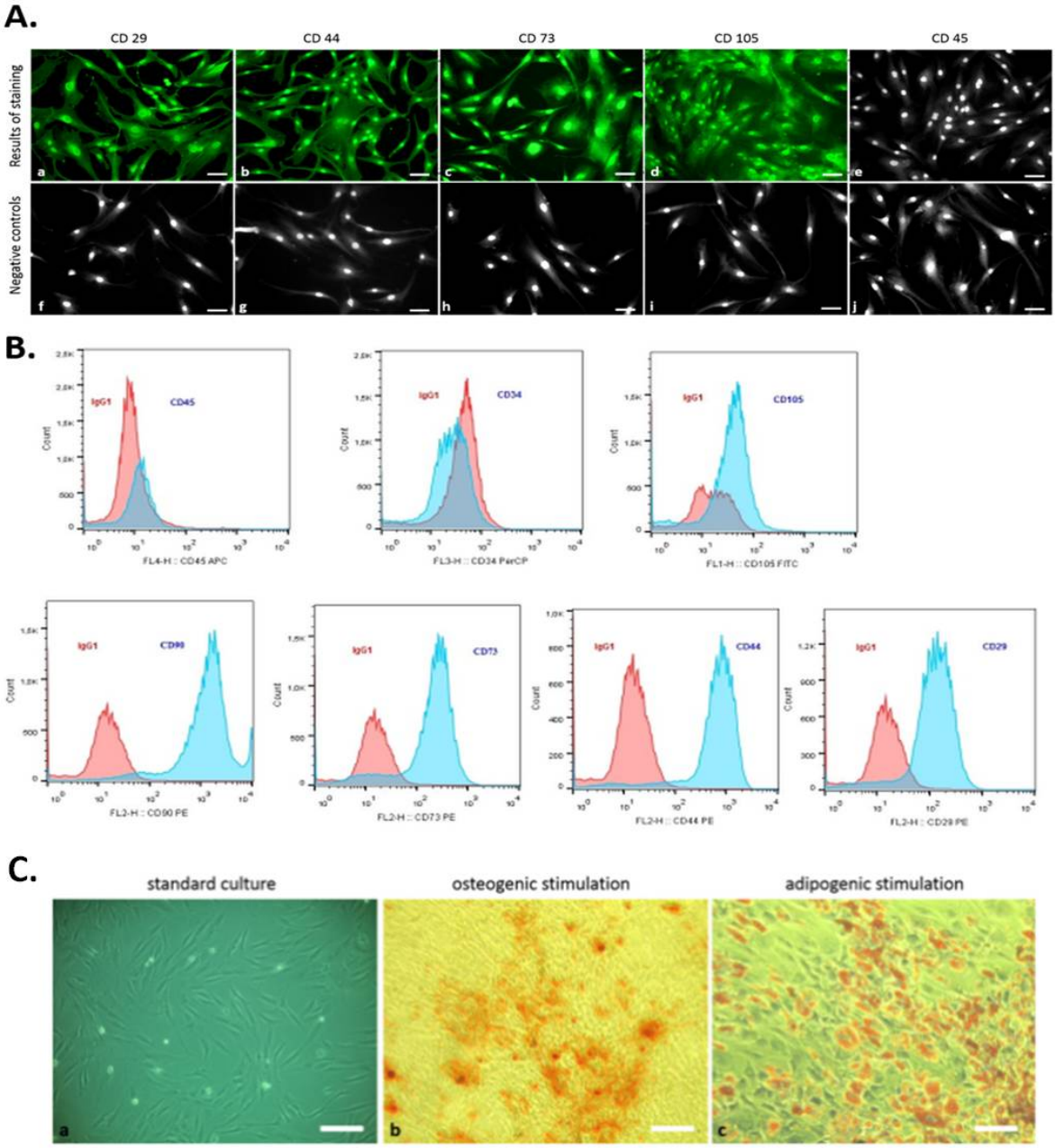


633

634 **Figure 2.** The expression of specific cell markers CD29, CD44, CD73 and CD105 and the lack of hematopoetic cell
635 marker CD45 (A). Characterization of hASCs FACS analysis. FACS histograms of passage 3 ASC simultaneously
636 stained for CD45, CD34, CD105, CD90, CD73, CD44, CD29, and IgG1 as negative control. Histograms are
637 representative of 3 independent flow cytometry analyses. Red histograms: IgG1 negative control; blue histograms:
638 antibody specific staining (B). Multipotency assay- standard culture and differentiated cultures after Alizarin Red

staining for osteogenic stimulation (mag. 50x, scale bar = 200 µm) and Oil Red O staining for adipogenic stimulation (mag. 100x, scale bar = 400 µm) (C).

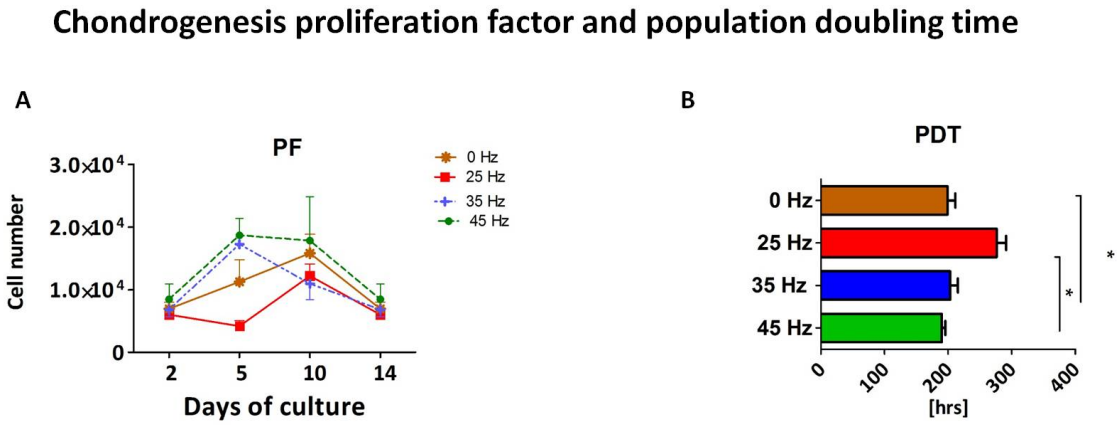


**Figure 3.** Proliferation factor (A) and population doubling time (PDT) (B) of hASCs treated with 0, 25, 35 and 45 Hz vibration frequencies during chondrogenic stimulation. * p-value < 0.05.

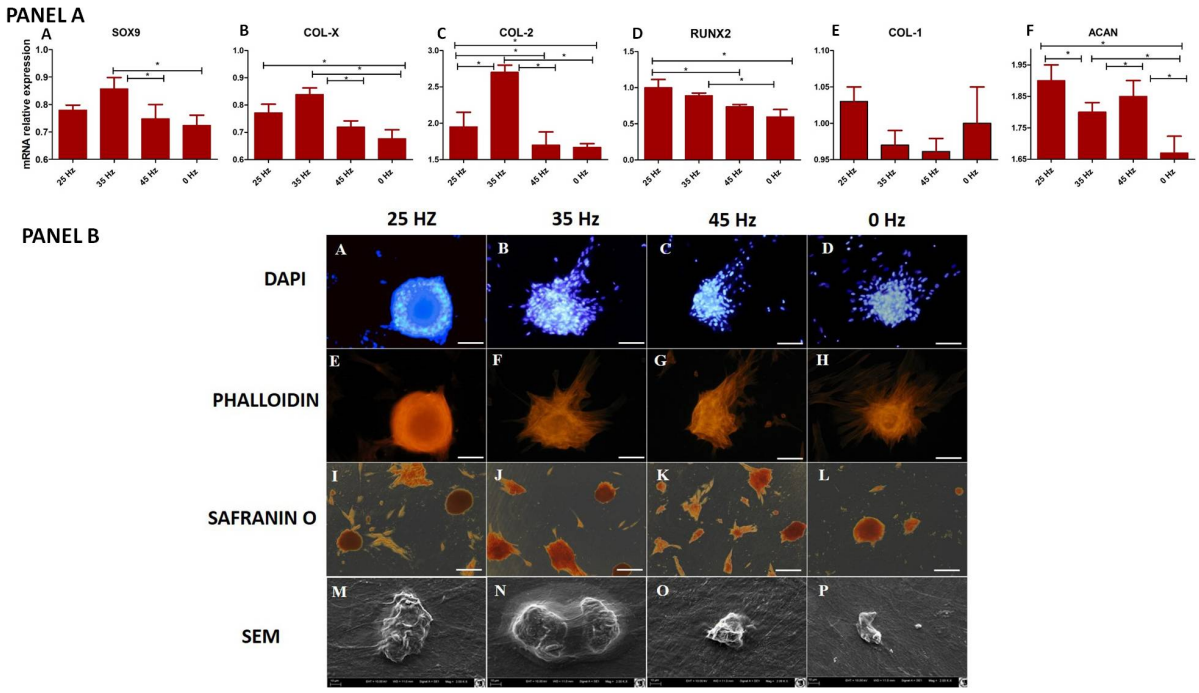


646

647 **Figure 4. Panel A** RT-qPCR for chondrogenesis genes: SOX9, COL-X, COL-2, RUNX2, COL-1 and ACAN from
648 hASCs that underwent chondrogenic induction on culture plates with treatment with 0, 25, 35, 45 Hz vibrations. * p-
649 value < 0.05 **Panel B** Cell morphology of chondroblasts originated from hASCs cultured on plates visualized by
650 fluorescence stainings (DAPI A-D and Phalloidin E-H), Safranin staining (I-L). Scale bars A-H 100 µm and I-L 200
651 µm and scanning electron microscope photographs (Mag. 2000x).

652

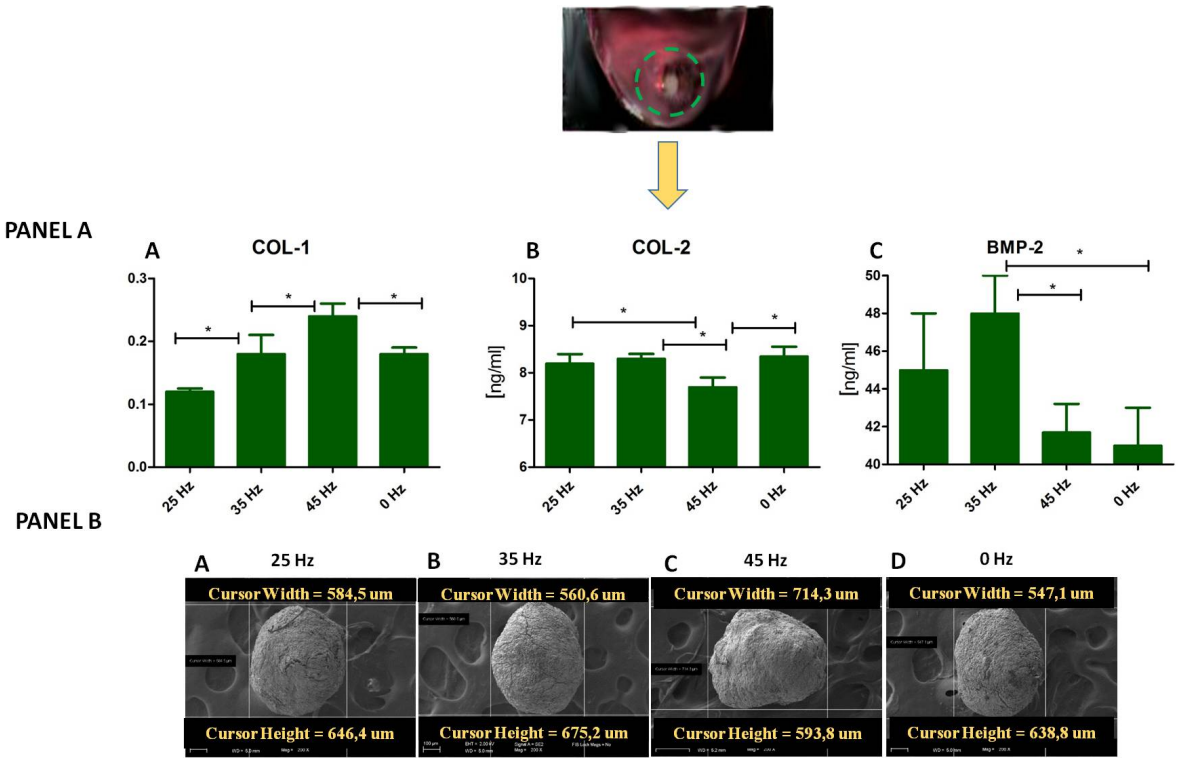


653

654 **Figure 5. Panel A** Comparison of Col-1 , Col-2 and BMP-2 levels by ELISA hASCs pellets after 14 days of
655 chondro-induction. **Panel B** Morphological characterization and comparison of chondro-nodules from cells cultured
656 at pellet.

657

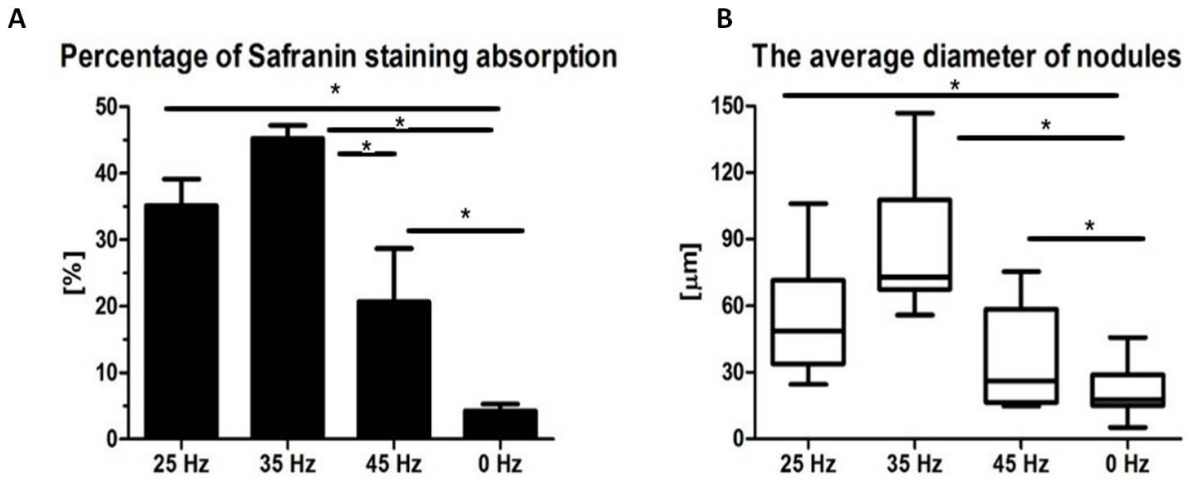


658

659 **Figure 6.** Percentage of Safranin staining absorption (A) and the average diameter of chondrogenic nodules (B)

660 from chondroblasts that originated from hASCs. * p-value < 0.05.

661

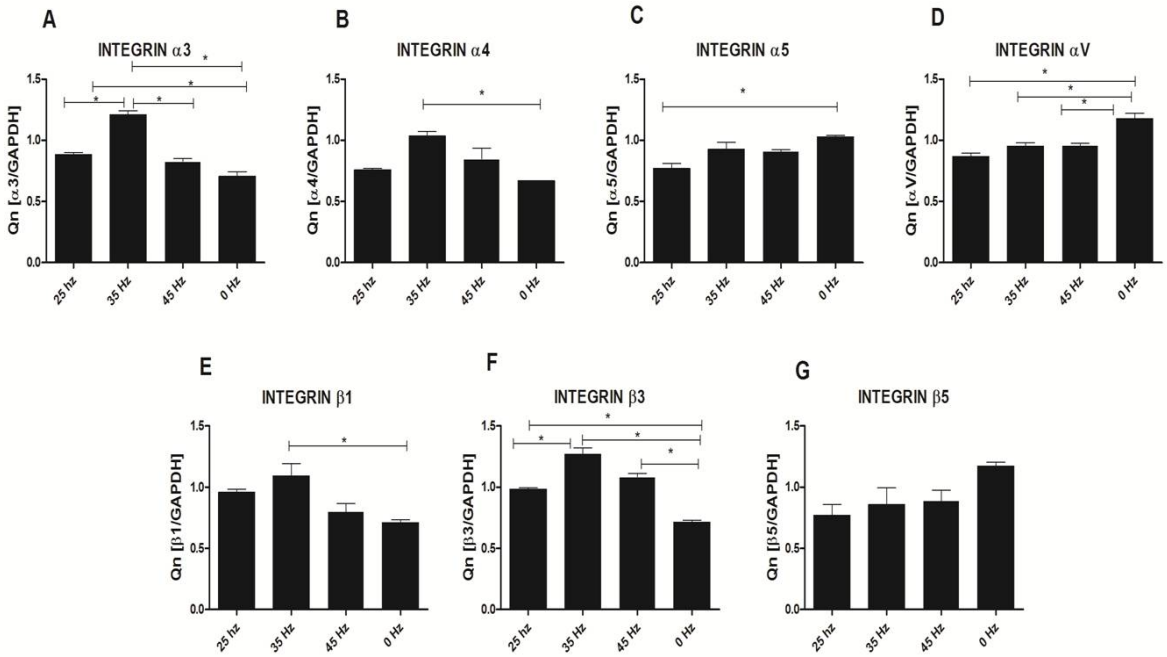


**Figure 7.** Integrin expression changes after mechanical stimulation of ASCs. Quantitative PCR analysis for integrin alpha 3, 4, 5, V and beta 1, 3, 5 subunits. *$p < 0.05$.

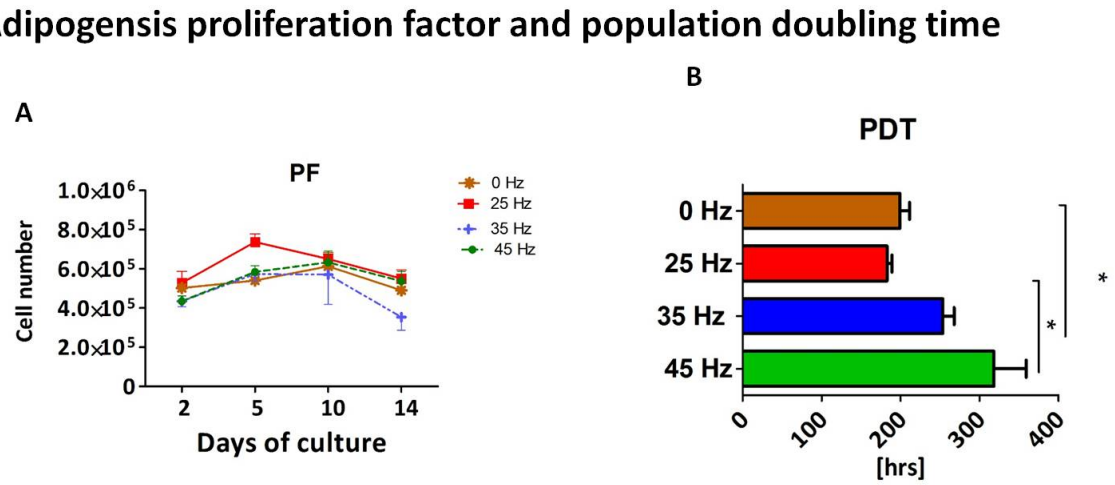


666

667 **Figure 8.** Proliferation factor (A) and population doubling time (PDT) (B) of hASCs treated with 0, 25, 35 and 45

668 Hz vibration frequencies during adipogenic stimulation. * p-value < 0.05.

669

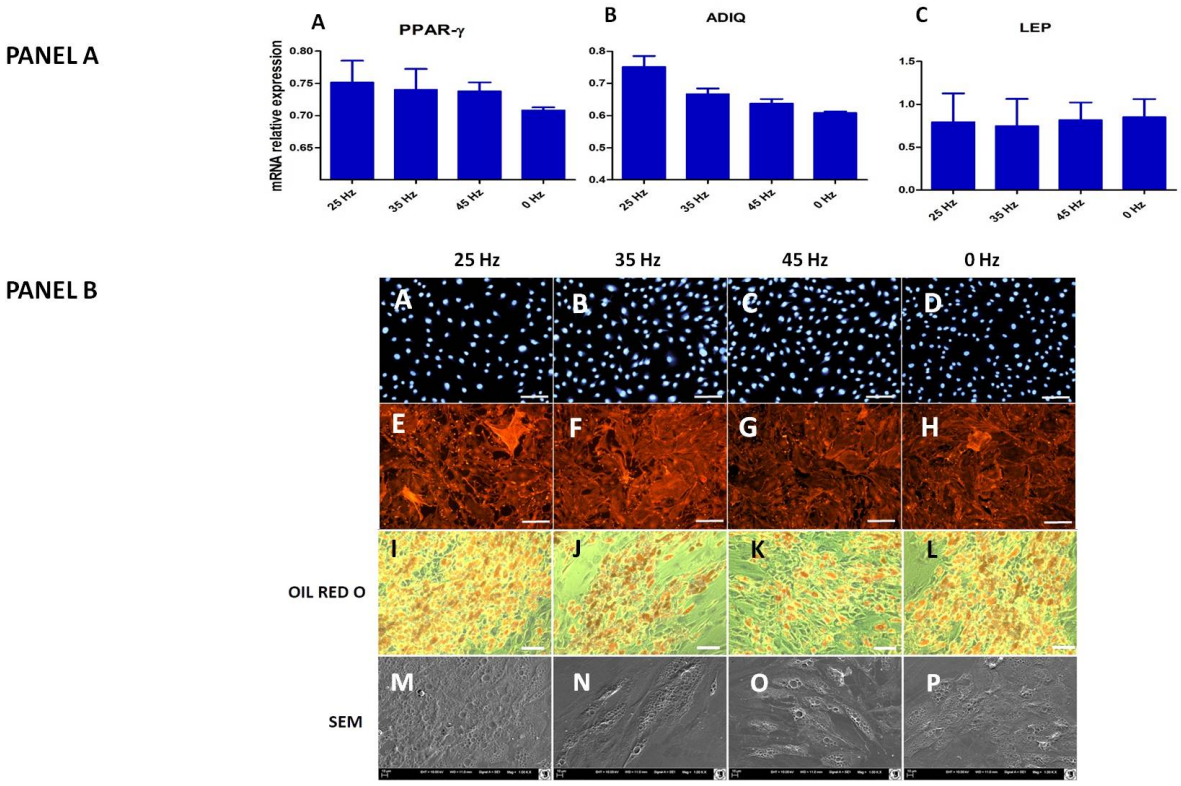


670

671 **Figure 9. Panel A** RT-qPCR for adipogenesis genes: PPAR-gamma, ADIQ, LEP from hASCs that underwent
672 adipogenic induction on with treatment with 0, 25, 35, 45 Hz vibrations. * p-value < 0.05 **Panel B** Cell morphology
673 of adipocytes originated from hASCs visualized using fluorescence stainings (Phalloidin, DAPI; Mag. 50x, scale bar
674 200 µm), Oil Red O Staining (100x, scale bar = 400 µm) and scanning electron microscope photographs (1000x).
675

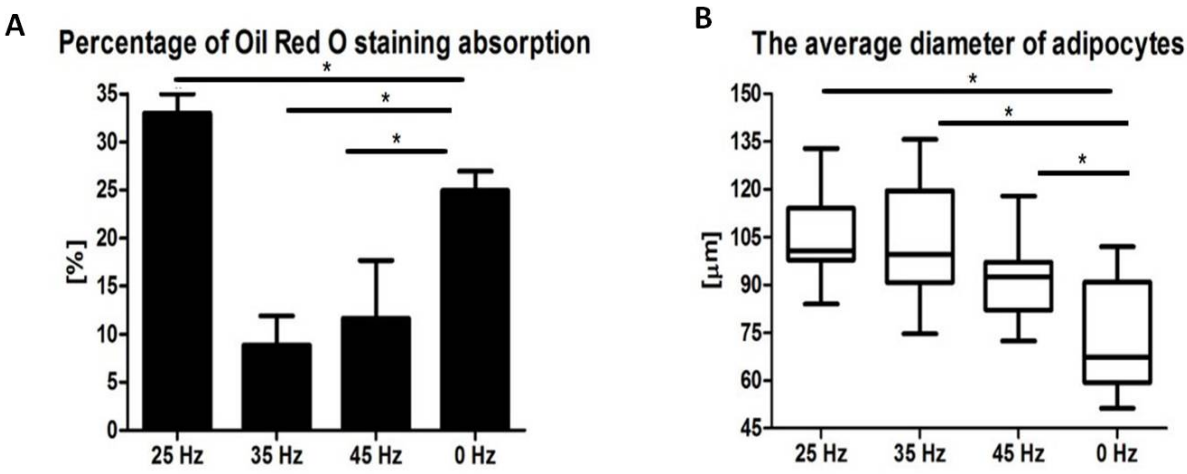


**Figure 10.** Percentage of Oil Red O staining (A) absorption and the average diameter (B) of adipocytes. * p-value < 0.05

# 1

Vibration generation prototype

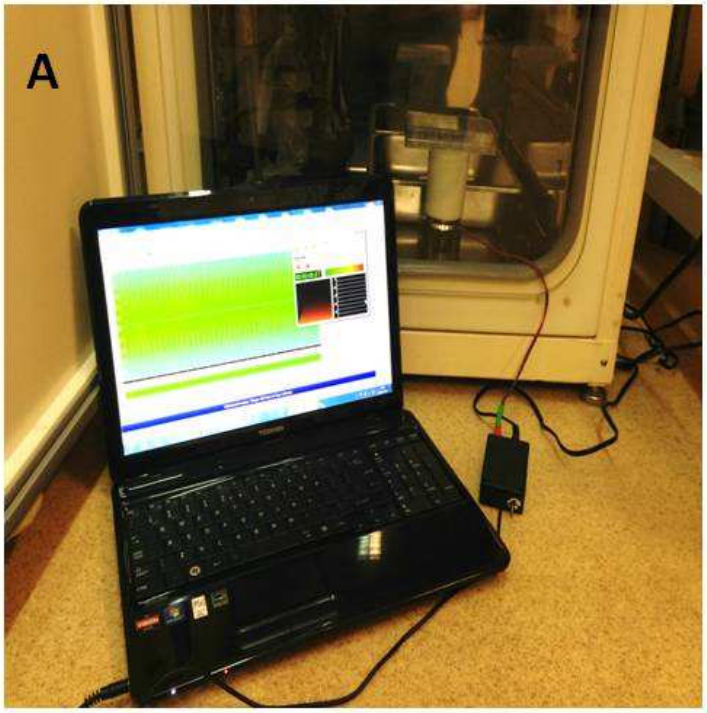


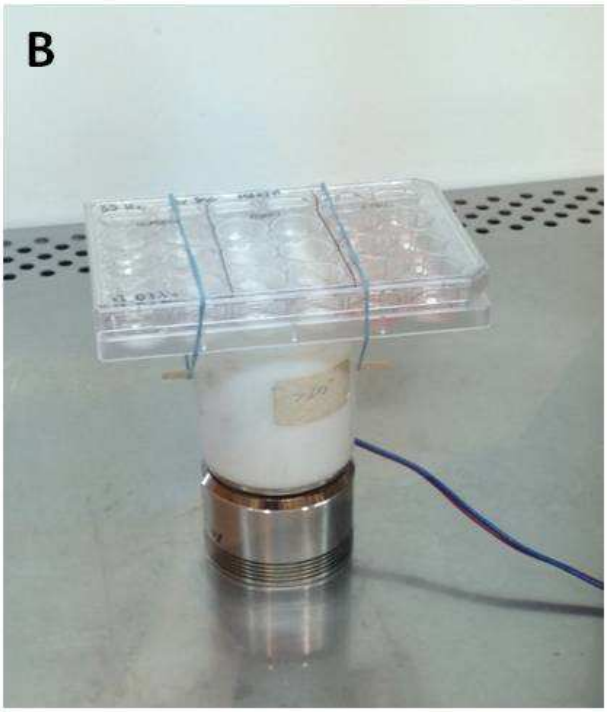


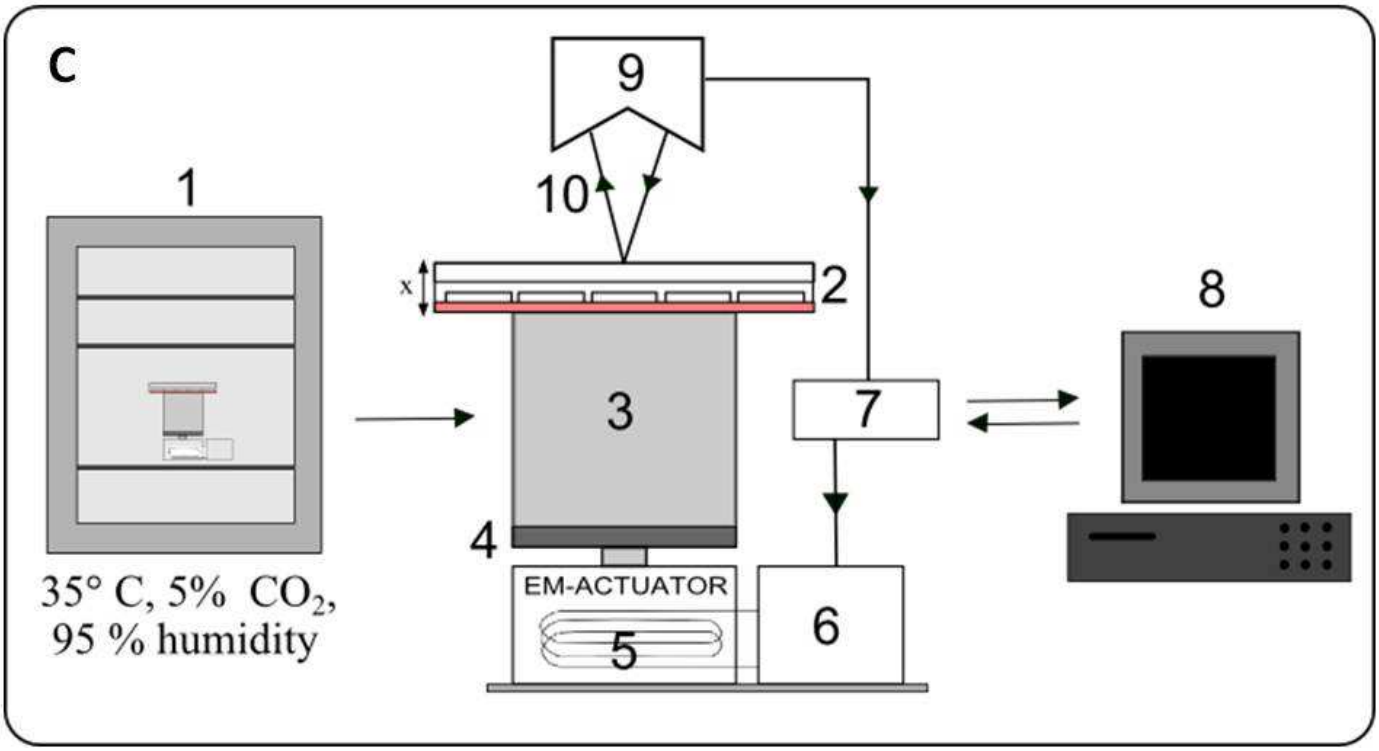


PeerJ PrePrints | https://dx.doi.org/10.7287/peerj.preprints.1514v1 | CC-BY 4.0 Open Access | rec: 17 Nov 2015, publ: 17 Nov 2015

# 2

## hASC phenotyping

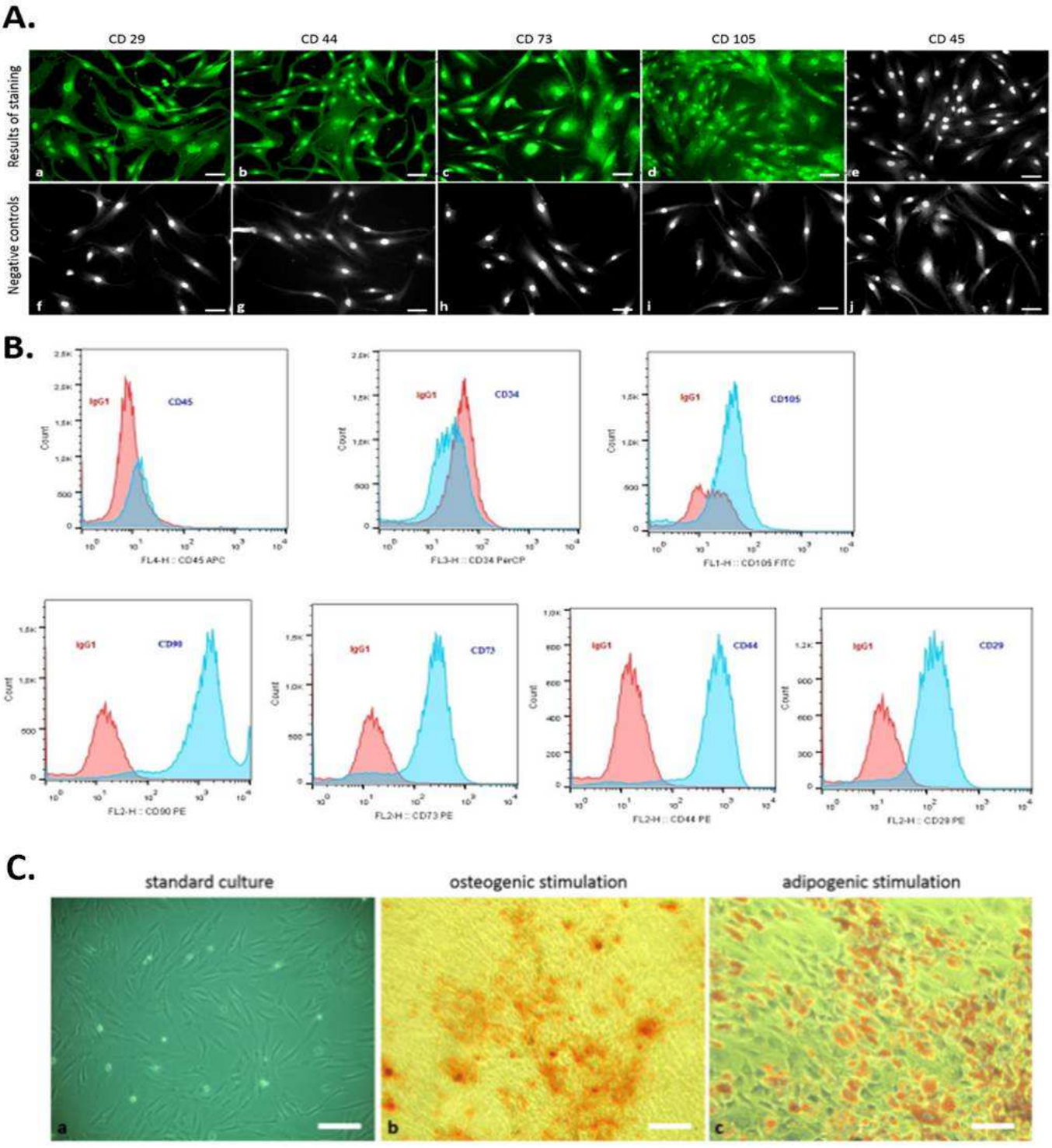

# 3

proliferation factor and PDT chondrogenesis

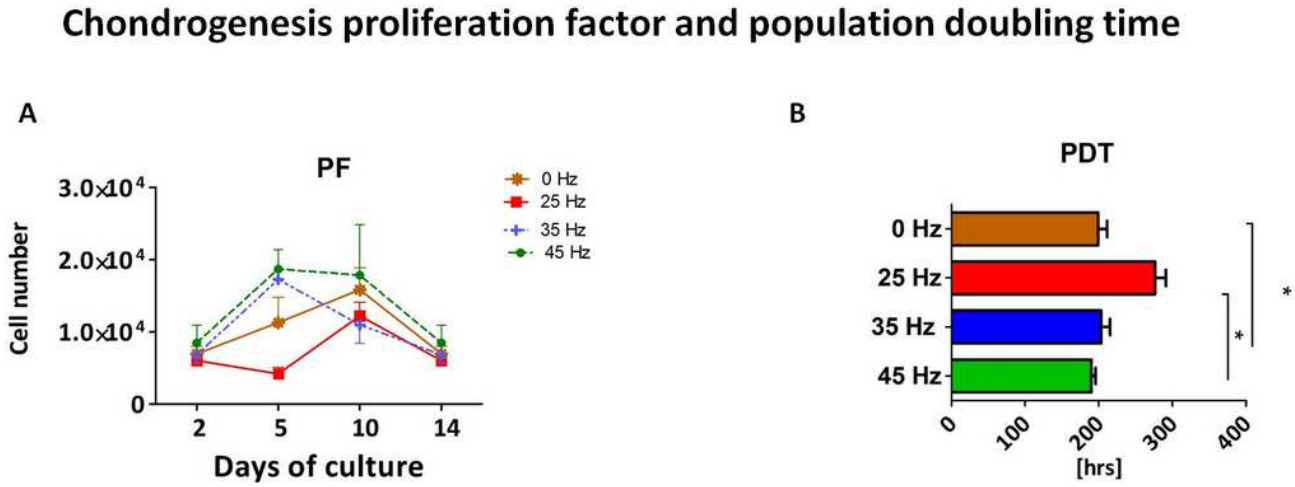

# 4

## qPCR and morphology chondroblasts

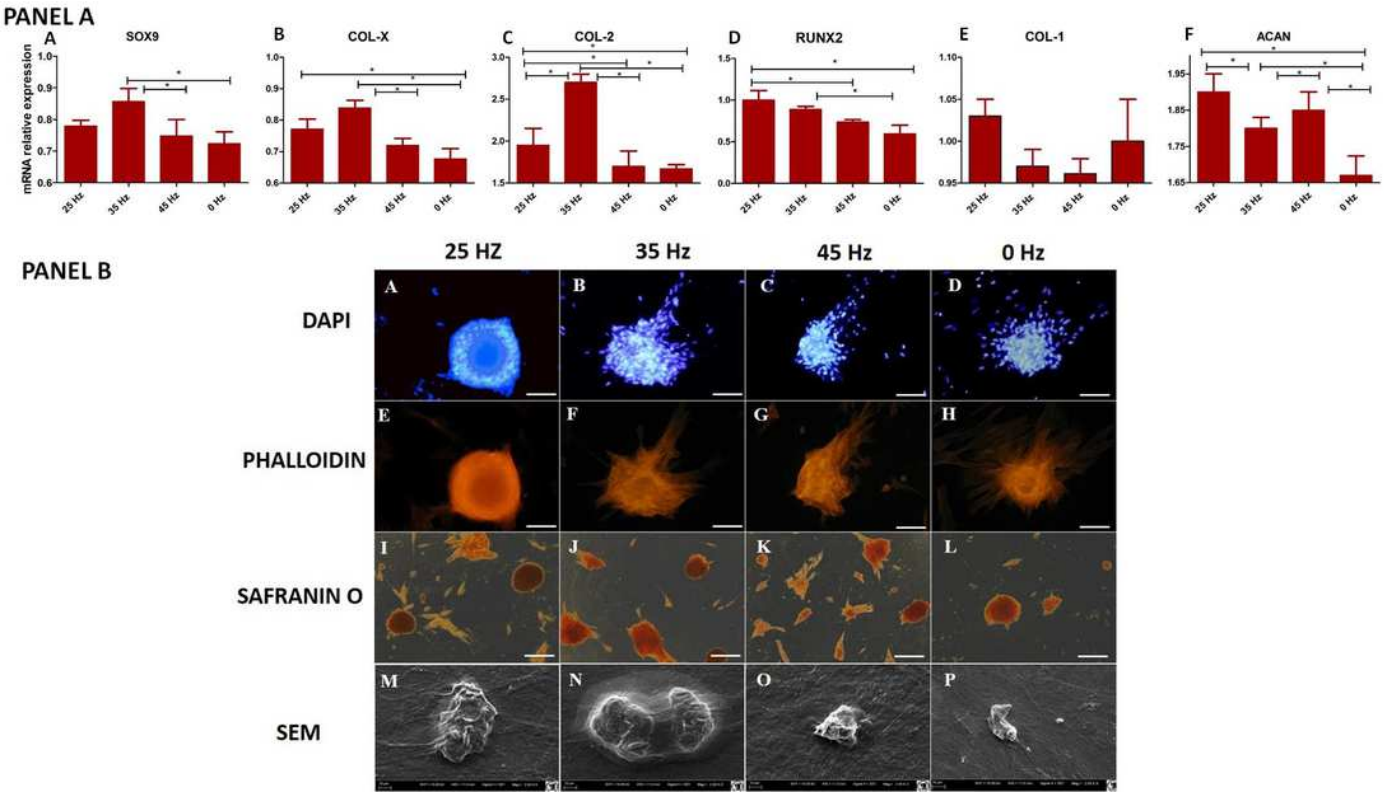

# 5

ELISA and chondro nodules

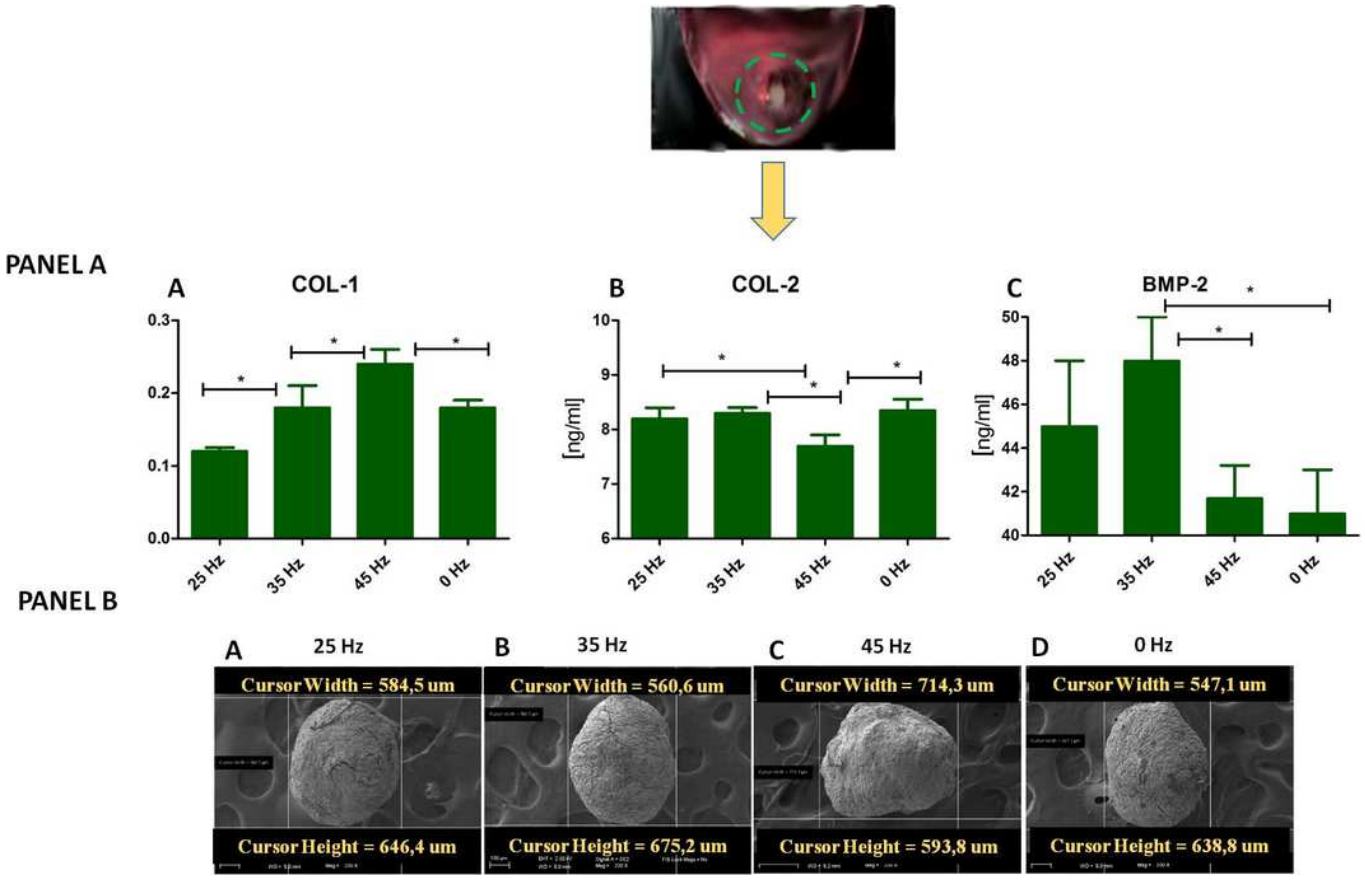

# 6

safranin absorbtion and diametres of chondronodules

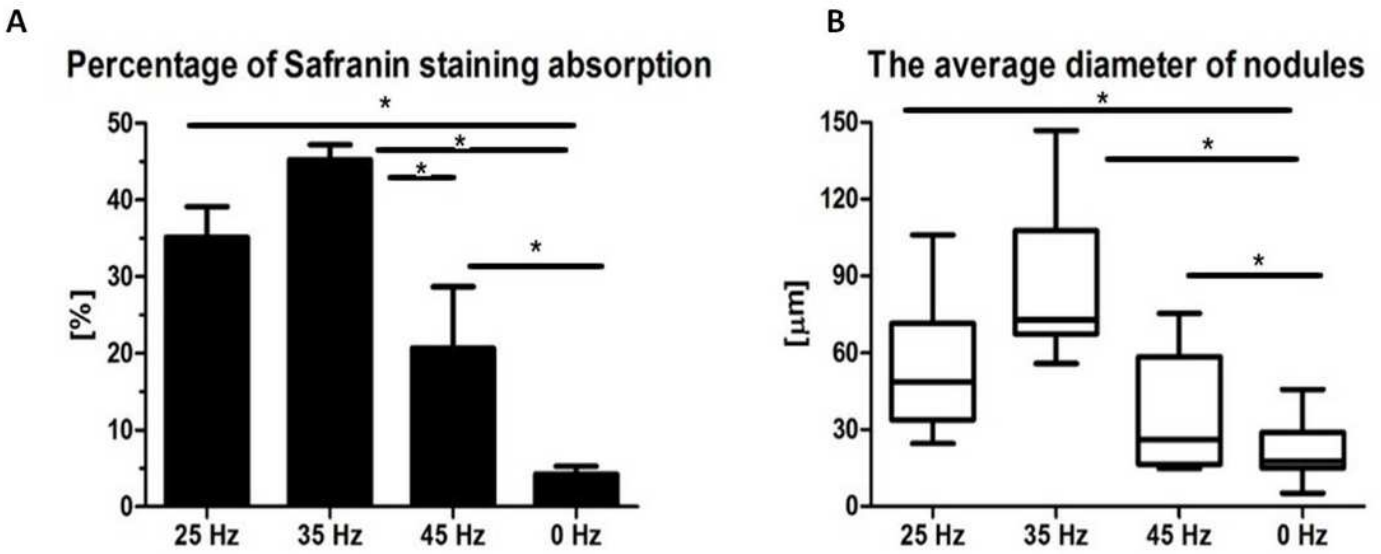

# 7

## Integrin expression (qPCR)

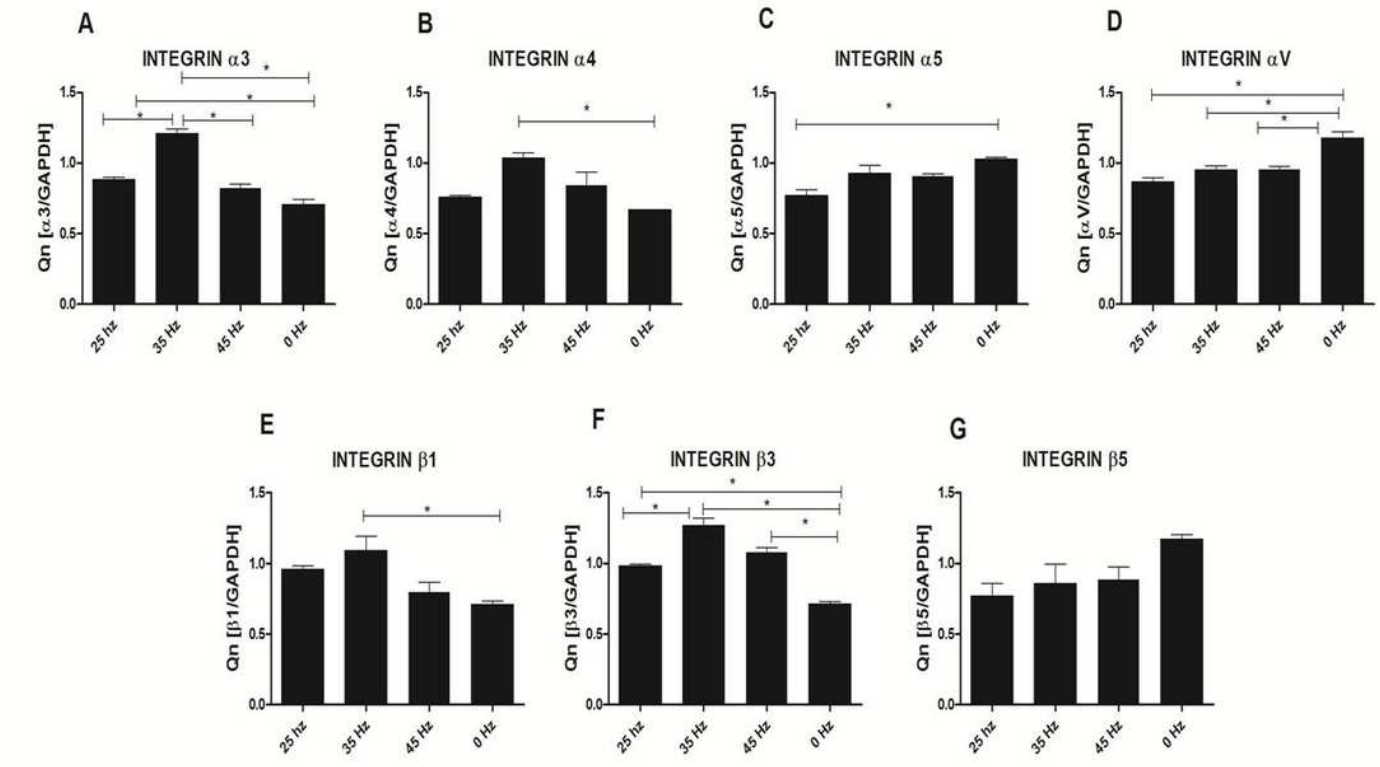

proliferation factor and PDT in adipogenesis

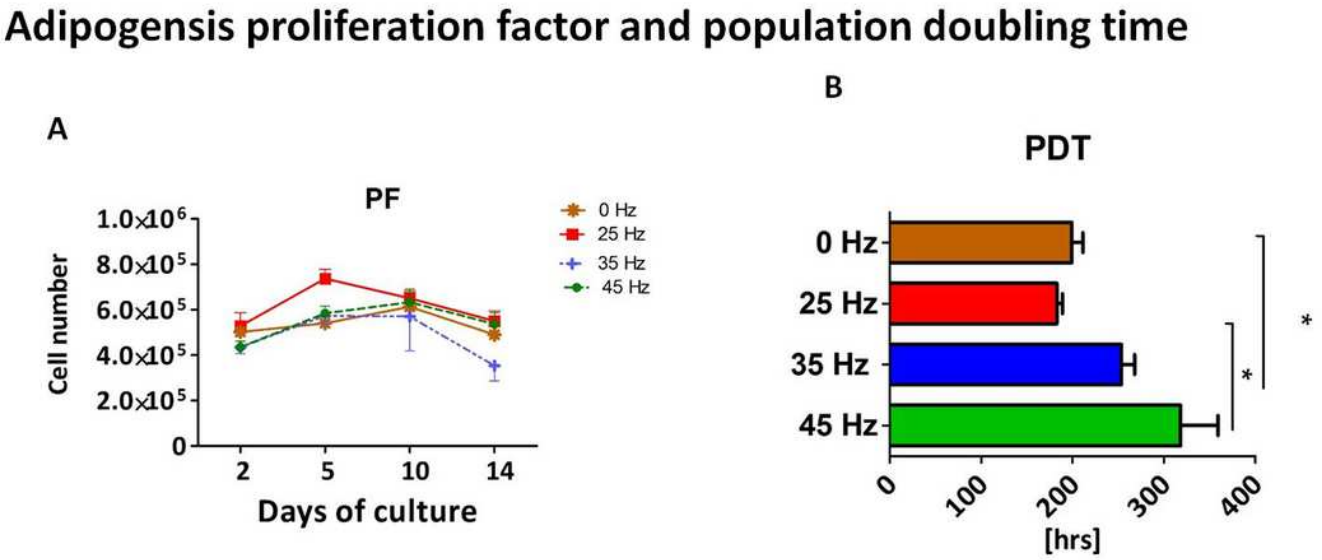

# 9

qPCR and morphology oof adipocytes

PANEL A

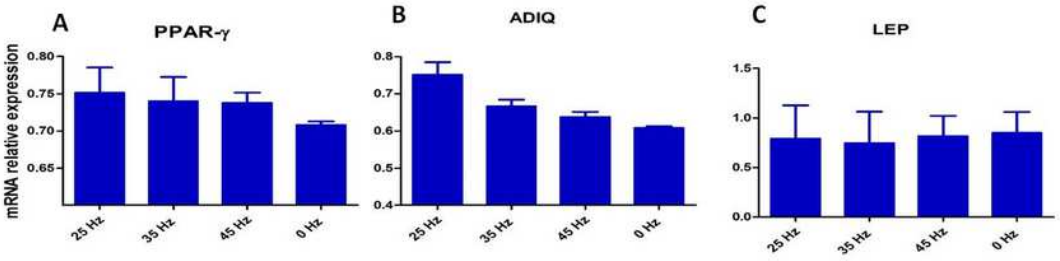


PANEL B

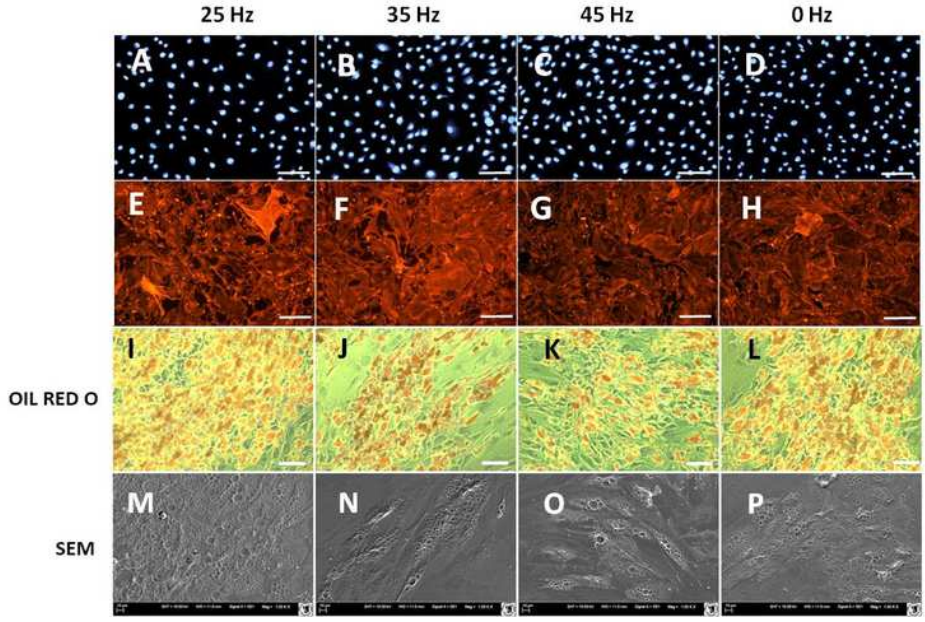

# 10

Oil red o absorption and adipocytes diameters